

The Relationship between Magmatic and Tectonic Processes in the Formation of the Oceanic Crust to the South of the Charlie Gibbs Fracture Zone (North Atlantic)

A. A. Peyve^{a,*}, S. Yu. Sokolov^a, A. A. Razumovskiy^a, A. N. Ivanenko^b, I. S. Patina^a, V. A. Bogolyubskiy^a, I. A. Veklich^b, and A. P. Denisova^a

^a *Geological Institute, Russian Academy of Sciences, Moscow, 119017 Russia*

^b *Shirshov Institute of Oceanology, Russian Academy of Sciences, Moscow, 117997 Russia*

**e-mail: apeyve@yandex.ru*

Received November 11, 2022; revised January 12, 2023; accepted January 20, 2023

Abstract—This article presents new data on the structure and relationship of tectonic and magmatic processes during the formation of the Mid-Atlantic Ridge between the Charlie Gibbs and Maxwell Fracture Zones in the North Atlantic. It is shown that this region is characterized by significant reduction in volcanism, which leads to the uplift of deep-seated rocks (ultramafic rocks and compositionally diverse gabbroids) to the seafloor surface. Both separate oceanic core complexes of the most varied configurations and extended sublittoral ridges composed of plutonic rocks are formed. Our analysis showed that this geodynamic regime exists during at least 14–16 Ma. The formation of most oceanic core complexes is associated not only with tectonic factors, but also with the serpentinization of peridotites, which leads to a decrease in density, an increase in volume, and, as a result, to the ascent of large ultramafic massifs, including disintegrated blocks of gabbroids, dolerites, and basalts. Numerous zones of sliding, crushing, abrasion, and deformation of rocks are evidence of tectonic movements. The area of study is characterized by numerous nontransform displacements of different amplitudes, which resulted due to relative displacements of oceanic lithosphere segments in wide areas under shear and extension conditions. The morphology of the forming tectonomagmatic structures is determined by tectonic factors. The exceptions are cases where the volumes of basalt melt that come to the seafloor surface for a short period of time are significantly higher than the average ones for a certain segment of the rift valley. The analysis we performed shows the presence of sources of heterogeneous magnetic anomalies both of volcanic origin and those associated with superimposed tectonic processes.

Keywords: North Atlantic, Mid-Atlantic Ridge, nontransform displacement, dry spreading, oceanic core complexes

DOI: 10.1134/S0016852123010053

INTRODUCTION

In accordance with the concepts of plate tectonics, the formation of a new oceanic crust in the Mid-Atlantic Ridge (MAR) was as follows. As the lithospheric plates diverge under the influence of mantle convection and crustal thinning, decompression melting of mantle rocks takes place in the area of maximum extension. The upwelling melts partially crystallize in the form of various gabbros in intermediate magmatic chambers and the bulk of the melts erupt on the seafloor surface, forming a new oceanic crust within the rift valleys of the MAR. As the plates move apart the newly formed oceanic crust as a part of the oceanic plates offset from the zone of its generation in the rift valley and the process is repeated cyclically. As a result, a system of basalt rift ridges sub-parallel to the rift valley axis is formed. In this case, the strikes of the spreading axis and the rift valley are perpendicular to the direction of divergence of the lithospheric plates. This structure is typical of most areas of the MAR.

The formation of individual spreading cells consisting of a rift depression and neovolcanic ridges and rises of different configurations is associated with the cyclic inflow of various volumes of melts and is determined by the degree of heating of the upper mantle rocks, the crustal thickness, and the amplitude of tectonic extension strain. Apparently, the extension deformations activate the cyclical outpourings of basaltic melts and the subsequent formation of the oceanic crust. The most kinematically stable configuration occurs when the strike of extension is perpendicular to the strike of the spreading axis in the rift segment. The strike of individual spreading segments of the MAR was emplaced at an early stage of the opening of the Atlantic and was determined by the distribution of stress fields at the initial stage of the breakup of continents. In some cases, however, the breakup occurred in such a way that the fault line without displacement had an arcuate shape and, therefore, spreading processes led to the formation of structurally more complex areas. In the oblique

spreading configuration, the strike of the axes of spreading segments of the rift valley is not orthogonal to the spreading direction [11].

In the rift valley, a system of second-order extension structures (depressions and neovolcanic rises) is formed, bounded by faults and strike-slip faults, the extension of which is orthogonal to the main tensile stress [16, 18, 39]. This is a relatively stable system that can exist for a long period of time. Nevertheless, changes in the relative direction and rates of plate movement can lead to changes in the spreading configuration in the axial part of the MAR.

In the Atlantic, oblique spreading is not a unique phenomenon. More than half of the rift segments of the MAR north of 15° N are structures that were formed under conditions of oblique spreading with an orthogonal deviation to the strike of the formed crustal segment by 10 or more degrees from the direction of divergence of the plates. Especially evident deviations are observed in the North Atlantic (Mohn and Knipovich Ridges and Lena Trough) [35].

Another significant factor that determines the structure of the oceanic crust forming in the MAR is the volumes of basalt melts outpouring onto the surface of rift valleys. In most spreading segments of the MAR, the volumes of incoming melts are sufficient to form a normal oceanic crust sequence at a low spreading rate, when deep-seated crustal or mantle rocks are not brought to the seafloor surface, even taking into account fault displacements. At the same time, isometric, sometimes dome-shaped uplifts, composed of deep rocks are formed in the areas where the volumes of the basalt melts are insufficient to form an oceanic crust sequence. They are usually located within the inner corner highs, i.e., in the conjunction zone of rift valleys with active segments of transform faults (where relative shear movements of oceanic lithosphere) so called oceanic core complexes [12, 17, 21, 31]. Their formation is associated with an extremely scarce transportation of basalt melts to the seafloor surface in the relatively cold conjunction zone between the rift valley and the transform fault.

Since extension and spreading occur regardless of whether basalt melts come to the surface or not, the extension in such areas leads to tectonic uplift of lower crustal and upper mantle rocks. Under extension conditions, this process occurs during the formation of low-angle faults, the planes of which are inclined towards the axis of the rift valley. If such conditions retain for a long time, then more complex structures are formed when a system of new low-angle faults cuts the formed oceanic core complexes [15, 36].

As detailed studies have shown, within the MAR there are several extended segments of rift valleys in which anomalous crust is formed without direct contact with transform faults. One of such segments (Sierra Leone) 250 km long is located in the south of Central Atlantic between 5° and 7°10' N [5].

The peculiarity of this segment is that there are no large faults with a significant displacement of a rift valley here, while it is not straight. The largest turns of rift valleys and related structures occur in two areas (6°15' N and 6°50' N). In terms of kinematics, they represent shear zones without complete rupture of rift structures. Such structures are known in other areas of MAR, these structures were called nontransform displacements (ND) [26, 41].

As evidenced from the morphology of structures and the ratio of different types of dredged rocks, the stratified sequence of the oceanic crust is almost absent in the Sierra Leone. The upper part of the oceanic lithosphere in this area consists of mantle ultramafic rocks with fragments of crystallized magmatic chambers (gabbros). The processes of tectonic emplacement of serpentinized to varying degrees mantle ultramafic rocks to the surface are fixed by melange and mylonitization zones in serpentinites. The basalt layer is practically absent.

The thin basalt flows form the lowermost part of the rift valley, pouring out onto serpentinized ultramafic rocks bearing gabbroid bodies. Such structurally complex zones, where deep mantle and lower crustal rocks are brought to the seafloor without forming the normal stratified sequence of the oceanic crust, were called amagmatic or dry spreading zones [6, 18, 28].

The similar structurally chaotic zone is traced from the Cape Verde Fracture Zone to the south for the distance of about 70 km [8, 13]. The similar areas are also known to the south of the Kane Fracture Zone (22°–24° N), where gabbro and ultramafic outcrops extend along the western side of the rift valley over the distance of 45 km [33]. The outcrops are confined to areas with a complex, irregular relief pattern, including numerous oblique seafloor scarps and rises.

These regions are characterized by the highest positive values of Bouguer anomaly, indicating a low thickness of the oceanic crust and a close position of dense upper mantle rocks. In addition, there is a good spatial correlation between the regions with thin oceanic crust (according to gravity data) and the distribution areas of ultramafic rocks.

Morphologically, such areas are characterized by a dissected relief, which is a complex combination of short highs and escarpments of various orientations formed as a result of significant tectonic movements.

The northernmost MAR segment, where dry spreading manifestations have been established, is the area south of the Azores (34°–38° N) [25]. Large dome-shaped massifs are described here, within five of which serpentinized peridotites were dredged.

The present paper aims to analyze new geological data, obtained during the study of previously unexplored MAR segment between the Charlie Gibbs and Maxwell Fracture Zones (North Atlantic), which was called Faraday after the name of the eponymous seamount located in its center and establishing patterns of manifestation and relationships between tectonic and magmatic processes during the formation of this structurally complex MAR segment.

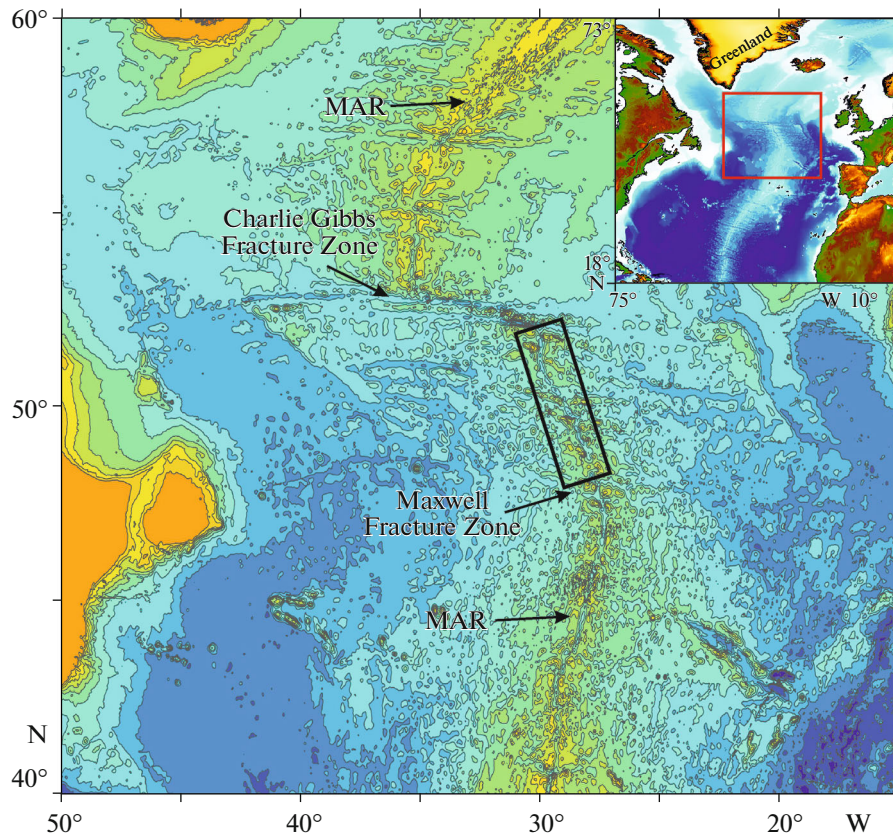


Fig. 1. The bathymetry map of the North Atlantic seafloor. In inset: the area of study (solid red line). In map: the area of detailed research (black rectangle).

THE STRUCTURE OF THE MID-ATLANTIC RIDGE IN THE FARADAY AREA

In 2022, within the framework of the Complex geological and geophysical studies of intraplate tectonic, magmatic and hydrothermal-metamorphic processes in the axial part and on the flanks of the Mid-Atlantic Ridge in the North Atlantic RAS program, the 53rd cruise of the R/V *Academik Nikolaj Strakhov* was conducted in the segment of the MAR between the Maxwell and Charlie Gibbs Fracture Zones (Fig. 1).

The field research included high-frequency acoustic profiling, magnetic survey and multibeam echosounder survey, as well as dredging. Data collection was carried out simultaneously by a Reson SeaBat 7150 echo sounder (Slangerup, Denmark) and a Edge-Tech 3300 profiler (West Wareham, USA). As a result, huge amount of data was obtained and added to previously obtained data on the morphology and material composition of structures in the Charlie Gibbs Fracture Zone area [9, 10, 38].

The analysis of the seafloor topography provides a key to understanding both the magmatic and tectonic processes that led to the formation of different structures of the MAR. According to the data obtained during the 53rd cruise of the R/V *Academik Nikolaj Strakhov* (Russia), a 1 : 50000 bathymetry map of the ocean floor was made, which, along with magnetic, high-frequency profiling, and dredging data, provided extensive geolog-

ical material to analyze the processes of formation of the oceanic crust of the extended (~500 km) MAR region (48°–52° N) south of the Charlie Gibbs Fracture Zone (Fig. 2).

The Faraday area includes very diverse in morphology and composition structures, which according to the set of peculiarities can be divided into five tectonomagmatic segments (TMS) (Fig. 3):

- TMS-1: between the Charlie Gibbs Fracture Zone and 51.2° N;
- TMS-2: between 51.2° N and 50.3° N;
- TMS-3: between 50.3° N and 49.7° N;
- TMS-4: between 49.7° N and 48.9° N;
- TMS-5: between 48.9° N and the Maxwell Fracture Zone.

THE STRUCTURE OF TECTONOMAGMATIC SEGMENTS OF THE FARADAY AREA

TMS-1: between the Charlie Gibbs Fracture Zone and 51.2° N

TMS-1 includes two structurally similar blocks, separated by a sublatitudinal linear depression, along which the northern block is displaced to the west relative to the southern one (Fig. 4).

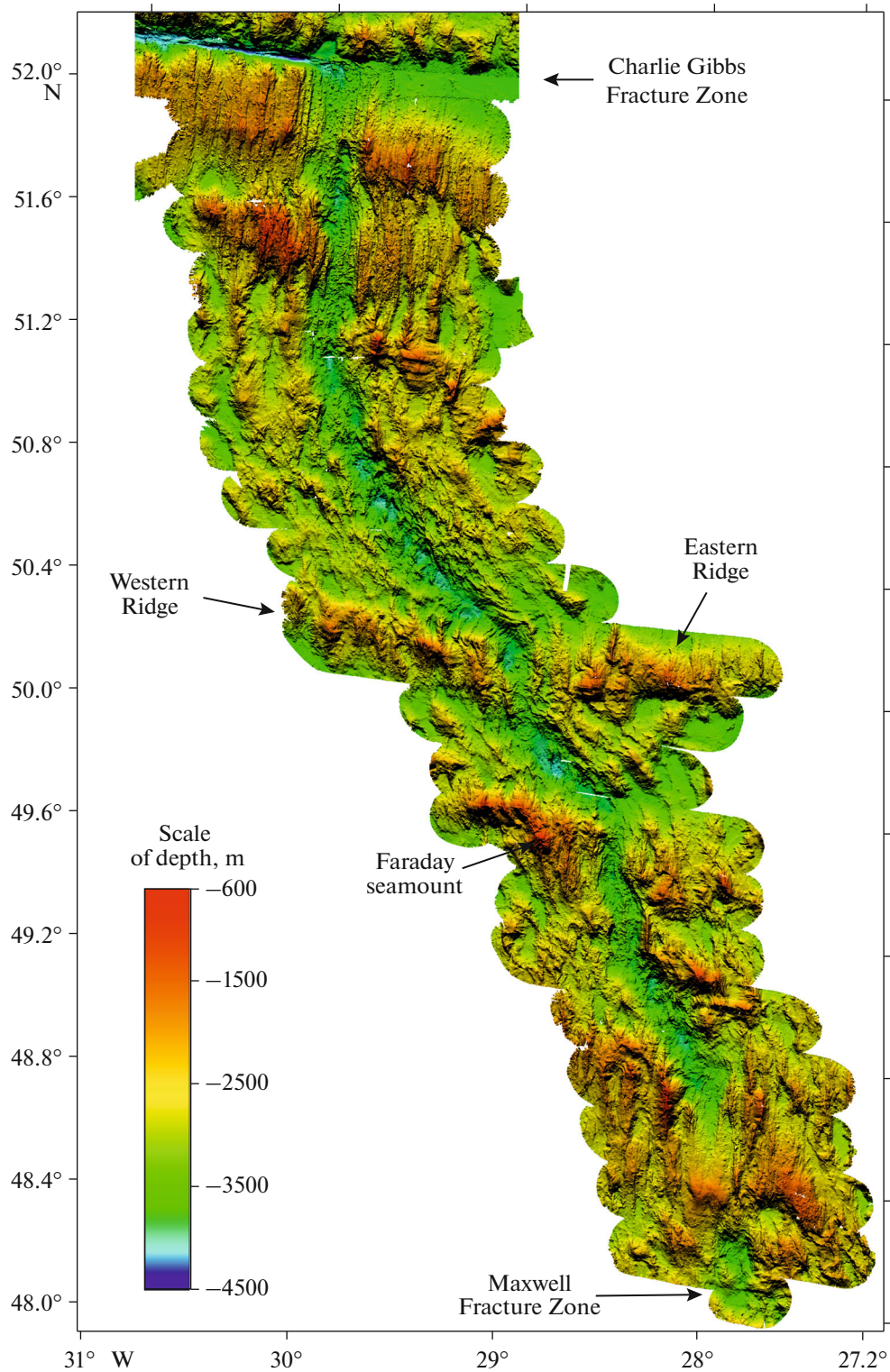


Fig. 2. The bathymetry map of the MAR seafloor in the Faraday area.

The rift valley is of 11–12 km wide and 3600 m deep within the northern block and extends along an azimuth of 5°. The valley bottom is flat. It gradually rises southward to a depth of 3200 m, which corresponds to the central part of the spreading cell, where the maxi-

imum volumes of basalt melts are generated and poured out (see Fig. 4 profile A–A').

Further to the south (at 51.8° N), the rift valley splits into two sub-parallel depressions with a shift relative to the rift axis, abruptly plunging to a depth of

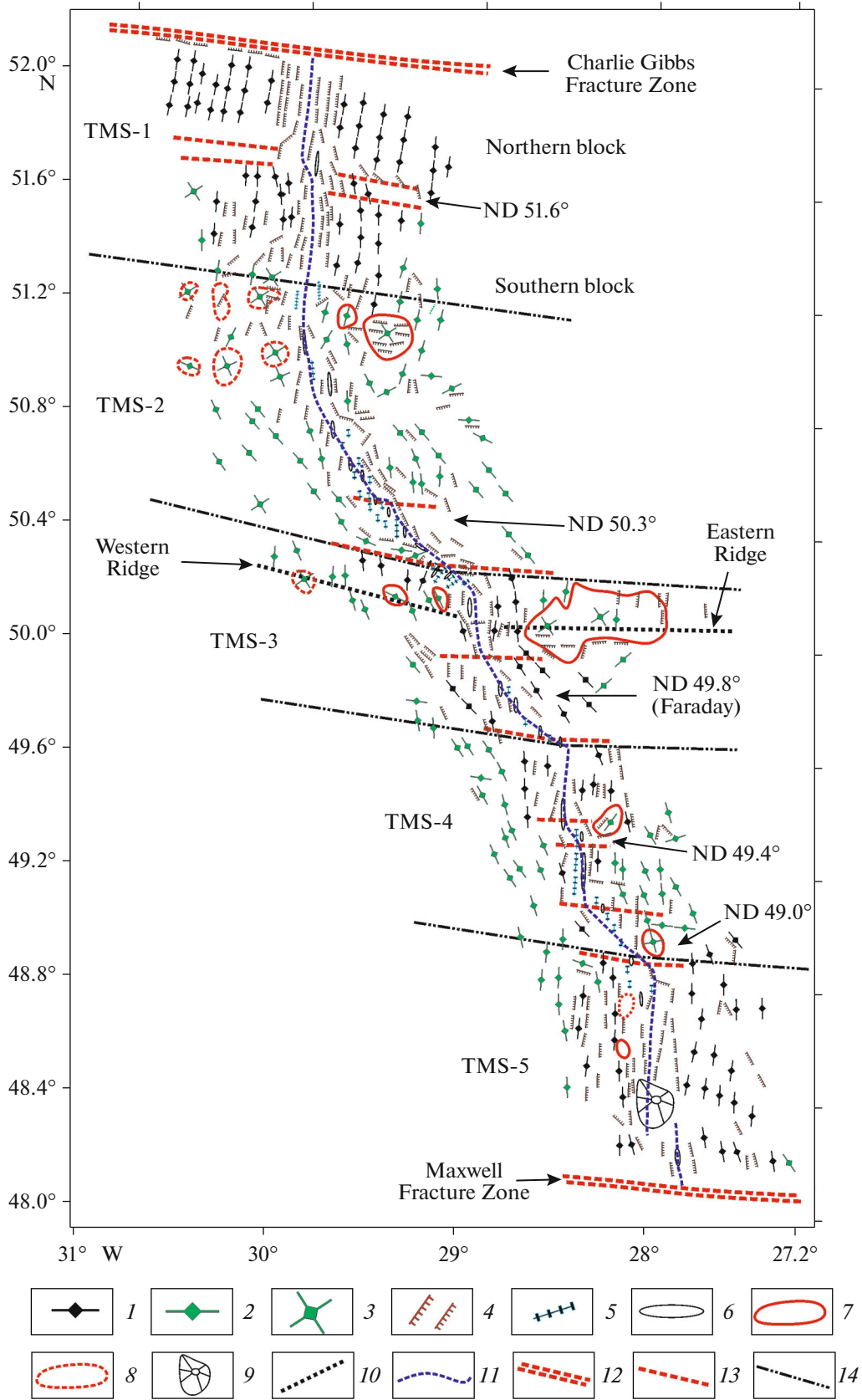


Fig. 3. The structural scheme of the Faraday area. (1–2) the strike of structures at flanks of the MAR rift valley of volcanic origin (1) and unknown origin (2); (3) isometric dome-shaped uplifts; (4) fault scarps; (5–6) structures of the rift valley: (5) neovolcanic ridges, (6) depressions; (7–8) distribution areas of deep rocks (gabbros, ultramafic rocks): (7) based on dredged data, (8) proposed; (9) dome-shaped volcanic edifice; (10) strike of sublatitudinal uplifts; (11) strike of the axis of the rift valley; (12) transform faults; (13–14) boundaries of nontransform displacements (13) and tectonomagmatic segments (14).

3600 m (in the western depression) and 4100 m (in the eastern depression). The neovolcanic ridge separating the depressions is oriented with a slight turn to the northeast. The sides are symmetrical, represented by steep extended fault scarps inclined towards the rift axis. According to dredging data, the rift valley is composed of fresh pillow basalts with a large volume of quenching glasses [7, 10].

The sublatitudinal linear depression, along which the northern block offsets relative to the southern one by 5 km, belongs to the group of nontransform displacements. Such structures could form both at the initial stage of the breakup of lithospheric plates and the change of the kinematics of their relative motion.

This nontransform displacement intersects the MAR axis at 51.6° N in an azimuth of 93° and is a U-shaped valley of 12–15-km wide and 2900–3200-m deep in cross section (locally overlain by sediments). The latter is crossed without displacement of the structure of both the rift valley and the framing rift ridges. However, while the height of the ridges in the central parts of the spreading cells reaches 1300 m, in the nontransform displacement the depths do not exceed 2300 m.

This is due to the fact that the lithosphere is colder at the margins of the spreading cells and the volumes of generated melts are essentially lower. There is another peculiarity. The western branch of the given nontransform displacement offsets to the north by 5 km together with the western flank of the northern block, which may indicate the existence of a shear component within the rift valley.

The rift depressions of the northern and southern blocks are echelon-like, with a slight overlap. This leads to an asymmetric spreading in the overlap area with an insignificant regular jump of the extension axis in the eastern (the northern block) and western (the southern block) directions. As a result, a serrated conjunction of rift seamounts formed in the northern and southern blocks is observed in the nontransform displacement area.

Rift ridges of both the northern and southern blocks are linear structures, which extend parallel to the sides of the rift valley by 20–30 km, separated by narrow troughs (Fig. 4; profile B–B'). The height of the ridges is 200–500 m from the base; the steepness of slopes is 10° – 22° .

Such structures are formed under normal spreading conditions, when the rift valley is orthogonal to the direction of divergence of lithospheric plates, and are composed of basalts. Each ridge corresponds to a formation cycle of oceanic crust, including the outpour-

ing of basalts at the rift valley bottom and the subsequent divergence and uplift of the valley sides with the formation of fault scarps and the subsequent formation of rift ridges.

TMS-2, between 51.2° and 50.3° N

The rift ridges of TMS-1 are rapidly submerging in the southern direction and discordantly jointed with several isometric or rounded dome-shaped rises. We draw the boundary between TMS-1 and TMS-2 along their southern foothills. Within the TMS-2, the rift valley gently changes its strike for a distance of 130 km from 5° – 6° to 310° , by more than 50° and rests on a rise at 50.3° N. The rise marks a sharp change in the strike of both the rift valley and rift ridges to a sublatitudinal one. This bend of structures can be considered as a nontransform displacement, which marks the boundary with the TMS-3. The rift valley axis is displaced eastward by 11 km without fracturing.

The structure of the rift valley of the TMS-2 differs significantly from the TMS-1.

The rift valley represents here a system of short echelon-like linear or isometric depressions 3–10 km long and the maximum depth of 4100–4200 m. They have a northern strike and are offset systematically in a southeasterly direction.

In the nontransform displacement area at 50.3° N, the southern depression is a festoon structure diverging into several linear apophyses-valleys of 3–7 km long. The latter turns fan-like from the southeast to the southwest to an azimuth of 300° in the youngest structures and rests on a sublatitudinal high at 50° N (Fig. 5).

This structure is formed in a shear stress field at local asymmetrical spreading, when each subsequent split occurs not in the center of the rift valley, but offsets in an easterly direction.

All intra-rift depressions are separated by a system of short narrow neovolcanic ridges with a height of 300–500 m from the base, which extend by 10–15 km along the strike of 4° – 5° . In the area of 50.9° N and 29.9° W is a 8×15 -km submarine volcanic plateau with separate distinct volcanic edifices, completely blocking the rift valley. The numerous single volcanic edifices are isometric in shape, about 1.8 km across at the base and 100-to-250-m high.

The sides of the rift valley are symmetrical: the average steepness of slopes is 20° – 25° . Despite the fact that the general strike of the rift valley sides corresponds to that of the rift axis, the lower parts of the slopes are terraced and dissected by a system of numerous small submeridional normal and strike-slip

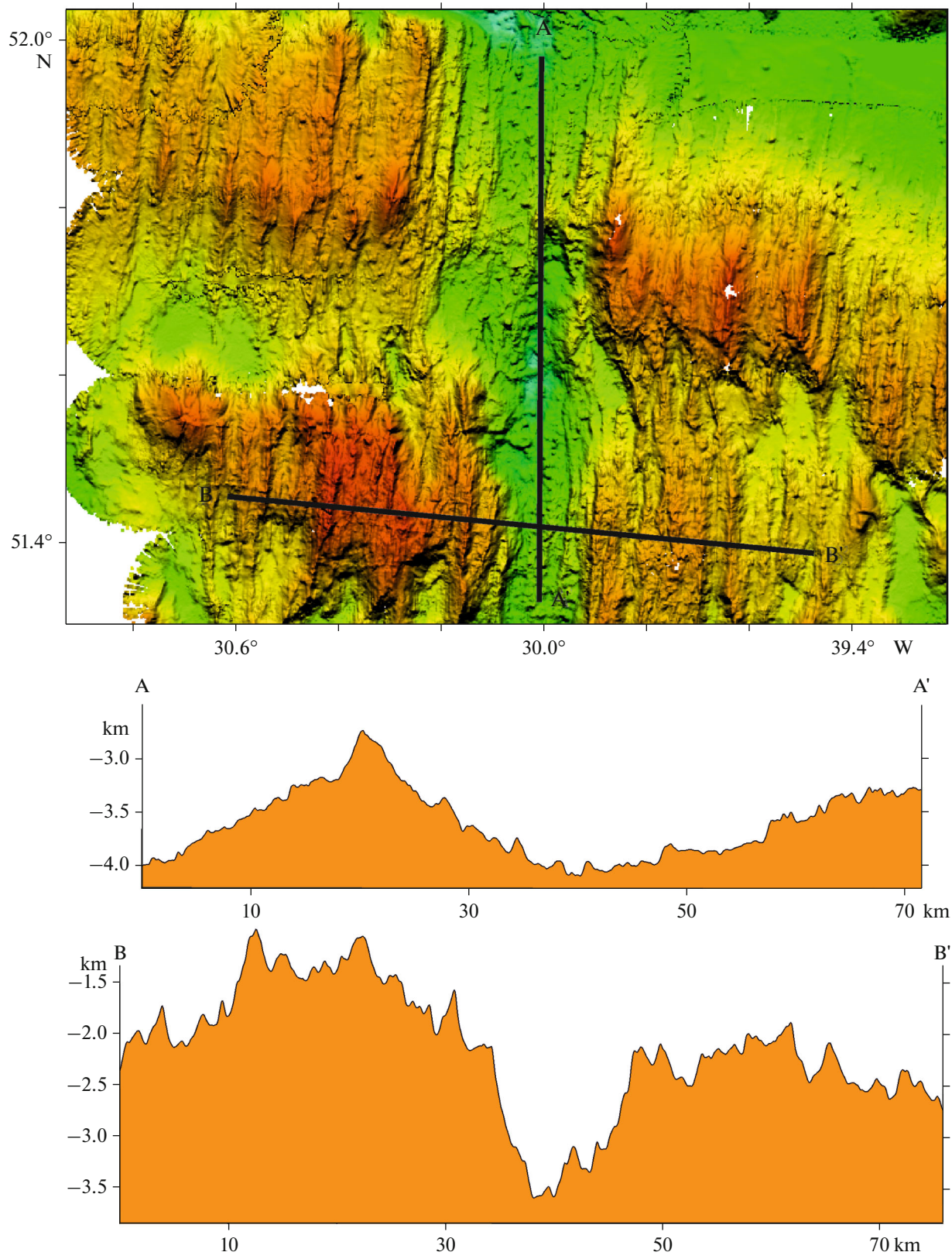


Fig. 4. The oceanic bottom topography and profiles in the TMS-1 area.

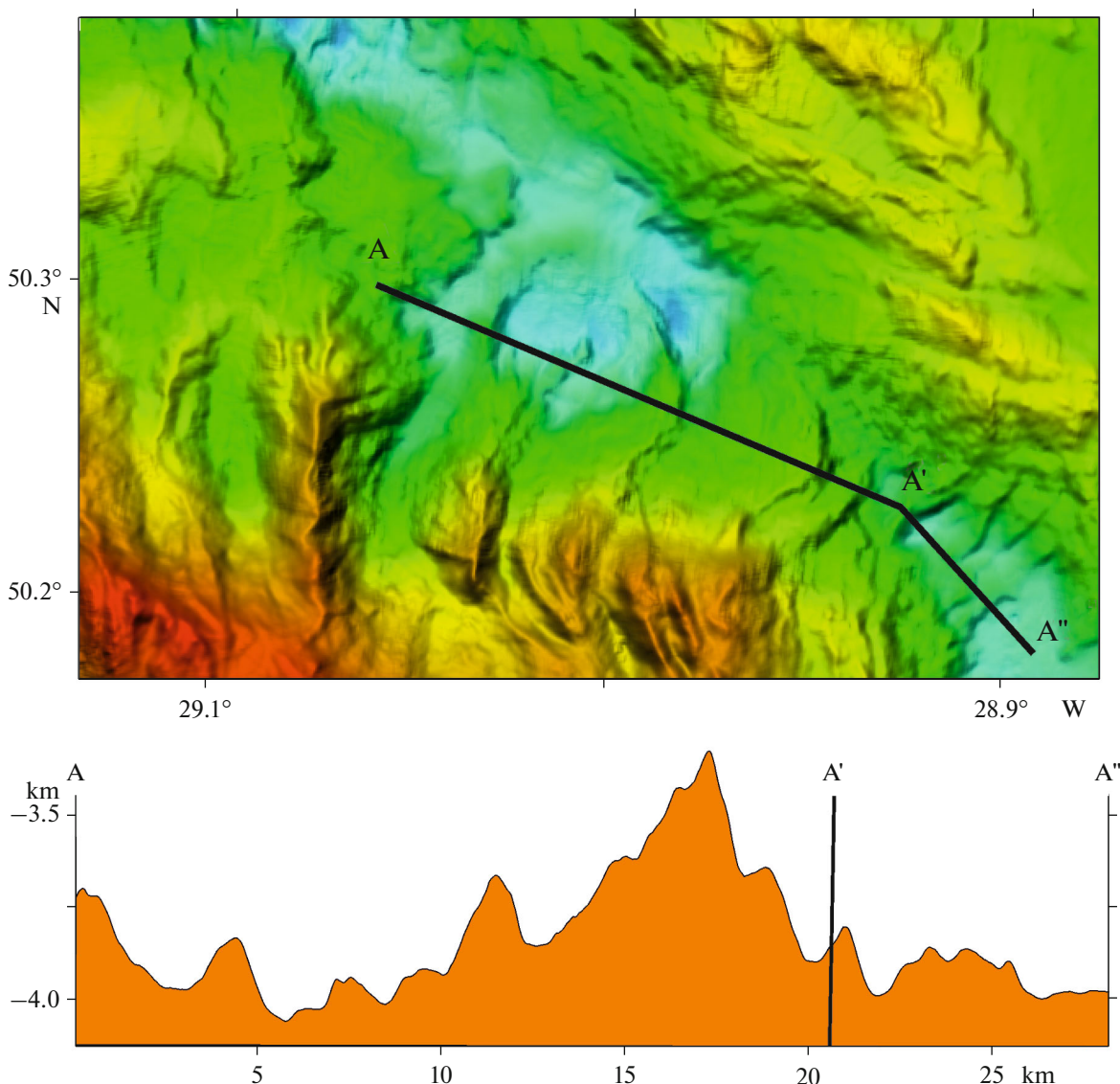


Fig. 5. The oceanic bottom topography and profiles in the TMS-2 area.

faults. The excess of the fault benches above each other varies from 10 to 100–120 m; the width reaches 700 m. Such structures are formed during oblique spreading, when the direction of divergence of lithospheric plates does not coincide with the direction of spreading.

TMS-2 is characterized by the absence of distinct extended abyssal hills. To the west and the east of the rift valley are individual linear and isometric rises with a strike from 6° to 330° on a plateau-like surface with depths of 3000–2900 m, forming small-ridge topography. The highest rises with summit depths of 750–2400 m are located in the northern part of the TMS-2. These are single ridges of 5–25 km long, separated by wide (5–7 km) U-shaped valleys. The ridges become narrower in the southern direction, ~500 m wide at the base. They are weakly expressed in topography with an excess of about 50–150 m from the bottom.

Rock samples were dredged on the largest rises to the east of the rift valley (Fig. 6).

One of these rises with a center at 51.15° N and 29.73° W is a narrow linear 15-km structure of about 6 km wide, extending along an azimuth of 6° , which corresponds to that of abyssal hills. The excess from the base is 1750 m. The high is asymmetrical. The steepness of the western slope is 20° – 25° that of the eastern slope is 25° – 45° . Dredging in the middle part of the southeastern slope showed that in addition to basalts and dolerites (65%), this structure is also composed of serpentinized mantle peridotites (35%). According to dredged rock samples, the latter were brought to depths of at least 2200 m. Thus, taking into account the depth of the rift valley of 3500 m at given latitude, the vertical displacement amplitude is at least

1300 m even without taking into account the fact that these are deep-seated rocks.

Another high with a center at 51.1° S and 29.5° W is an isometric, brachymorphic uplift with minimum depths of about 1500 m, within which are sublatitudinal different-sized flat-topped ridges with a strike of 278°, resembling a corrugated surface (see Fig. 6, profile B–B').

According to dredging data, one subrounded basalt block of unclear origin was raised from the high on the southwestern slope at depths of 2200–1900 m. The rest of the dredged rocks is represented by ore taxitic and pegmatoid gabbros with a large amount of ilmenite and sphene. Corrugated surface of slopes can correspond to tectonic scratching [14, 30].

The morphology and composition of rocks of this rise are similar to those of oceanic core complexes, formed during the tectonic uplift of deep-seated rocks to the seafloor, when the volume of outpouring basalt melts was not enough to form a normal oceanic crust sequence or there were extended intervals between basalt outpourings.

Here, one can observe a distinct asymmetry relative to the axis of the rift valley. There are no such large rises on the western flank as on the eastern flank. To the west of the rift valley there are a number of rounded dome-shaped uplifts with summits of 2400–2200 m, as, for example, the rise at 50.97° N, 30.41° W (Fig. 6, profile A'–A").

These structures were not sampled. However, as evidenced from the morphology, they are significantly different from rift ridges of volcanic origin and can largely consist of deep rocks and to be tectonic in origin.

TMS-3, between 50.3° N and 49.7° N

A large sublatitudinal ridge 15–20 km wide in the northern part of TMS-3 is divided by a rift valley into Western and Eastern branches (Fig. 2).

South of 50.2° N, the rift valley abruptly changes its strike to 355° (the axial rift depression proper is up to 7°). It coincides with the strike of extension axis (Fig. 7). This orthogonal segment stretches south for 25 km to 49.9° N.

At the intersection with the sublatitudinal ridge, the rift valley narrows to 7 km and its depth decreases sharply from 4100 to 3375 m. However, already at 50° N, the valley expands sharply to 21 km and deepens again to 4000 m. The valley bottom is strongly dissected. Numerous volcanic edifices up to 1.5 km across and up to 180 m high occur (see Fig. 7, profile A–A").

Starting from 49.9° N, the strike of the rift valley changes again to 311° and then does not change up to 49.7° N.

The rift valley in this area consists of several submeridional depressions separated by large neovolcanic linear ridges that cross the entire rift valley bottom in

azimuths 356°–358°. They offset en echelon to the southeast, following the structures formed under the conditions of oblique spreading. The total eastward displacement of the rift valley axis is 25 km. This structure can be considered as a large nontransform displacement. It is known as the Faraday transform fault [23]. However, there is no displacement of the rift valley at the intersection of this structure, and it is located, like the previous displacements, nonorthogonal to the strike of the rift valley axis.

The flanks of the TMS-3 are asymmetrical. The western flank is represented by low-ridge relief, which is similar to inland structures of the rift valley in morphometric parameters and northern strike. At a distance of 15–20 km from the margin of the valley, the low ridges are replaced by large massifs oriented in a north-westerly direction, i.e., following the strike of the rift valley itself. These massifs are 20 km at a width of 7–8 km; their relative height reaches 1050 m. Separate craters and calderas occur within the massifs. The latter are separated from each other by depressions up to 6-km wide, with a leveled bottom.

The eastern flank of the spreading segment consists entirely of similar large massifs, similar to the massifs on the western flank in morphometric parameters and north-western strike. However, their outlines are smoother here and the summit tops are predominantly rounded. The excess of the massifs above the bottom of the depressions separating them reaches 1300 m.

There are also isolated calderas and craters here, but in smaller numbers than on the western flank. The width of the depressions separating the massifs reaches 12 km. The low-ridge topography described on the western flank is practically absent on the eastern one. It is possible that some of these massifs may be composed of deep-seated rocks.

The sublatitudinal ridges are located between a non-transform displacement of 50.3° at the northern margin and a nontransform displacement of 49.8° (Faraday). They extend in an azimuth of 286° (Western) and 88° (Eastern) for a distance of 200 km and 135 km, respectively (see Fig. 7, profile B–B').

Judging by the extent of the Western sublatitudinal ridge and the extrapolation of linear magnetic anomalies [32], the formation of these structures in this setting has continued for at least 14–16 million years. Moreover, while that of the Eastern Ridge, as a whole, corresponds to the direction of spreading (the difference is only about 3°), the difference at the Western one is 21°.

The ridges are represented as a combination of meridional ridges and massifs formed at the merging of several short ridges reaching depths of 1300 m. Ridges and massifs are asymmetrical with more gentle slopes facing the rift valley. Small latitudinal ridges form corrugated surfaces on these slopes. One can also observe asymmetry in the meridional direction. The northern slopes of the western ridge are steeper, whereas

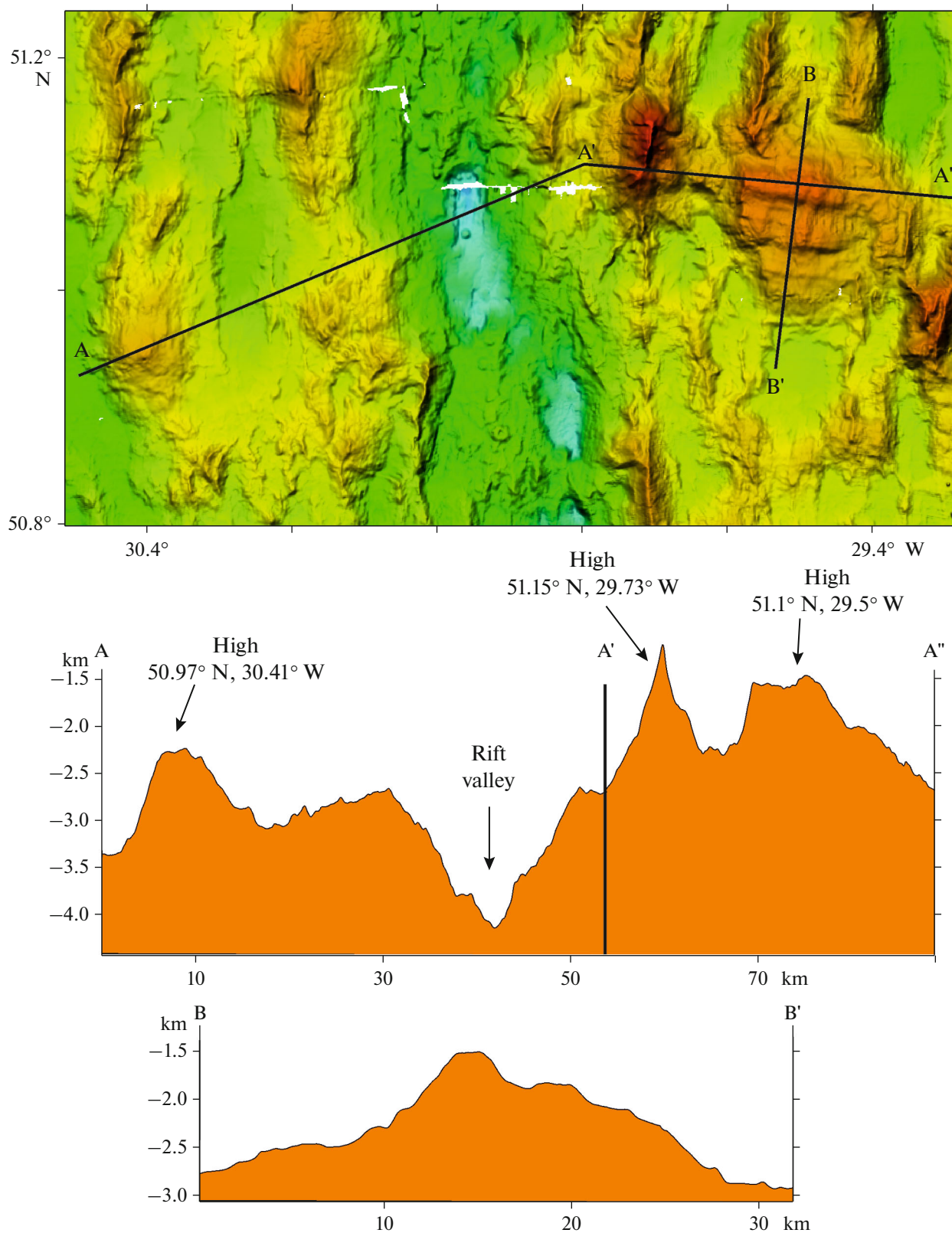


Fig. 6. The oceanic bottom topography and profiles across the structures of oceanic core complexes.

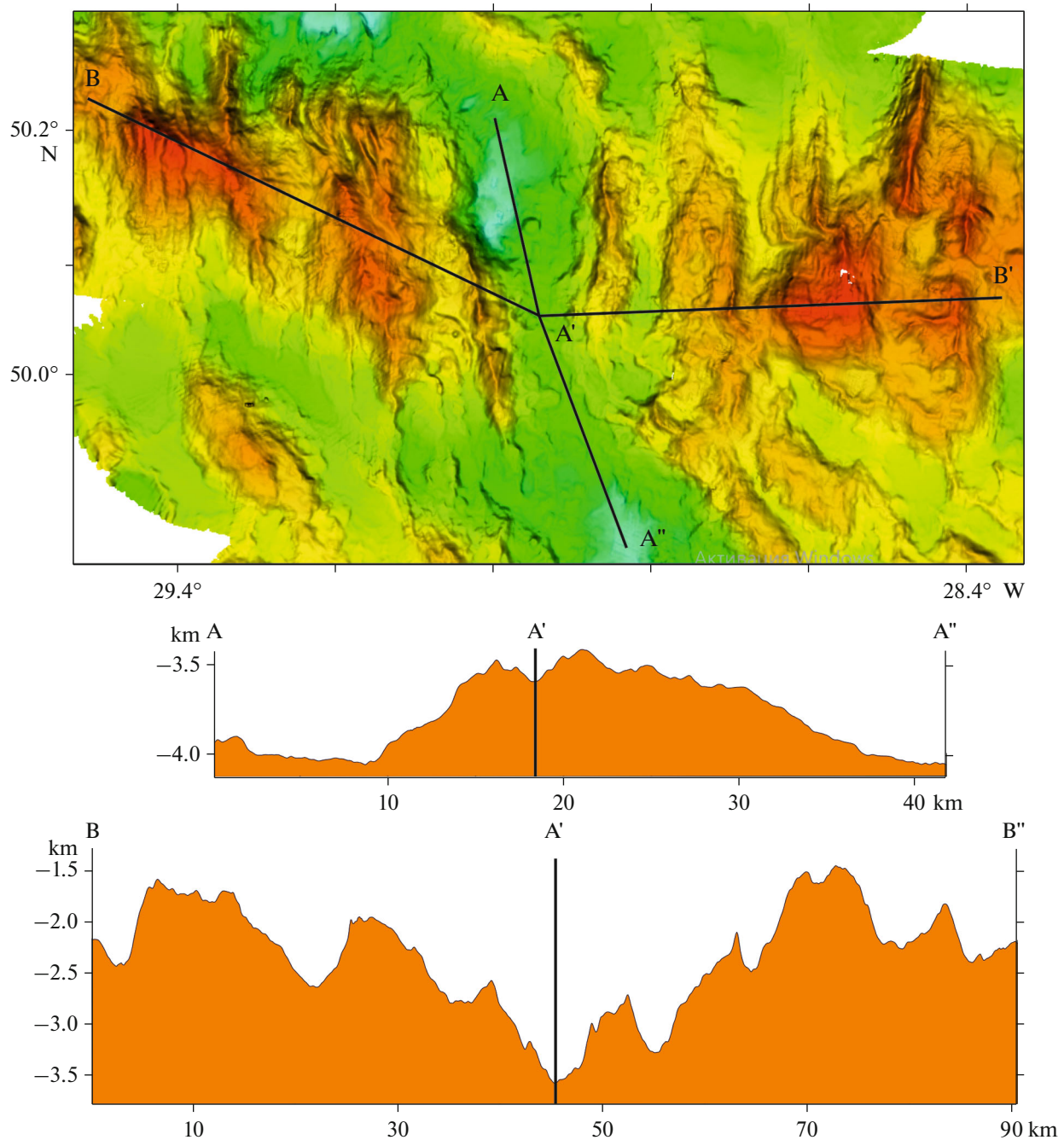


Fig. 7. The oceanic bottom topography and profiles in the TMS-3 area.

the eastern ridge shows the opposite situation. The length of the ridges varies from 5 to 18 km at the width from 2 to 6 km. The massifs are up to 20 km long and up to 25 km wide. The summit planes are rounded, less often represented by narrow ridges.

According to dredging data (nine dredgings), the Eastern Ridge is composed mainly of serpentized and tectonized ultramafic rocks (70%). Gabbros make up ~25%, basalts and dolerites are 5%. Basalts and dolerites that predominate within the Western Ridge

make up 75%, Gabbros make up about 20%, and ultramafic rocks are 5%. Thus, there is an asymmetry both in morphology and in the composition of the rocks of the Eastern and Western Ridges at a distance of 60 km away from the axis of the rift valley.

TMS-4, between 49.7° and 48.9° N

This segment extends in the southern direction from the southern boundary of the Faraday nontrans-

form displacement (49.7° N) to 48.9° N and includes two meridional segments of the rift valley, separated by small nontransform displacements (Fig. 3):

(i) the northern nontransform displacement 49.4° (49.42° – 49.36° N) with the offset of the rift valley to the east by 4 km;

(ii) the southern nontransform displacement 49.0° N (49.1° – 49.93° N) with the offset of the rift valley to the east by 17 km.

South of the Faraday nontransform displacement, the rift valley changes its strike from 311° to 4° . The segment of the rift valley is 28 km long and 10–12 km wide at the smallest width in the central part. Here, the bottom of the valley is most elevated to a depth of 3300 m (Fig. 8, profile A–A").

Numerous cone-shaped volcanic edifices are observed. The diameter of individual volcanic cones varies from 600 to 1300 m, with a height from 40 to 70 m. The slopes of the valley are stepped, symmetrical; their average steepness is 15° – 20° . The nontransform displacement of 49.0° with the general north-western strike of the rift valley is divided into several elongated rift depressions separated by large volcanic ridges 5–7 km wide and 12–20 km long and 500–600 m high from the base. The strike of these structures in the rift valley is 3° – 7° . The steepness of the slopes represented by fault scarps reaches 35° – 40° . This structure of the rift valley corresponds to the kinematic situation of oblique spreading.

The greatest diversity in structures is observed beyond the rift valley.

Between 49.7° N and 49.3° N are large ridges of abyssal hills and isometric, rarely elongated along the rift valley strike massifs, superimposed on the ridged topography. This topography dominates clearly on the eastern flank and only two large massifs, composed mainly of ultramafic rocks and separated by depressions are distinguished. Here, the western flank consists almost entirely of massifs merged into a single ridge 65 km long (Fig. 8, profile B–B'). One of these massifs is known as Faraday seamount [23]. Apart from basalts and dolerites, this ridge is composed of deep rocks (gabbros).

The ridged topography is characterized by picked ridges of up to 22 km long, up to 2.2 km wide, and up to 300 m high; the strike is 352° . The ridges are asymmetrical. The slopes facing the rift valley, as a rule, are steeper. On the eastern flank of the valley, the ridges are separated by inter-ridge depressions up to 3-km wide. On the western flank, the ridges are separated only by narrow (the first hundreds of meters) ravines (Fig. 2).

Massifs are usually rounded, from 8 to 10 km across. The slopes are also asymmetrical. The slopes facing the rift valley are gentler. There is also an asymmetry in the north–south direction. Its character is similar to that previously considered within TMS-3 (the northern slopes are steeper). The summit surfaces

are uneven. There are isolated small volcanic edifices within the separate massifs. The strike of the ridges of the western flank is submeridional, while the massifs themselves have a different strike. Some dredgings showed that the massifs are largely composed of deep-seated rocks (gabbros and ultramafic rocks).

The morphology of the western and eastern flanks differs between 49.3° N and 48.9° N. The eastern flank is characterized by the ridged topography of abyssal hills. Except the ridge closest to the rift valley, all other ridges have a small height not exceeding 150 m at a width of 1.5–2 km. Their strike is about 350° , which corresponds to the average strike of the rift valley axis. The length of the ridges ranges from 8 to 10 km.

The ridges do not connect with the massifs located to the north at 49.4° N being separated by a ravine 100–150 m deep. As well, the ridges are also separated from each other by small ravines or depressions up to 3 km wide. One can observe separate craters and calderas varying in diameter from 1.5 to 17 km within the ridges. The ridge up to 600 m high and 3.5 km wide closest to the rift valley stands out separately.

To the south, the ridges merge into a large massif with a height of 1500 m from the base, consisting of several rounded and sublatitudinal highs, some of which are composed of serpentized mantle ultramafic rocks. The total strike of the massif is 286° .

The western flank is characterized by longer winding ridges (from 10 to 17 km). The width of the ridges varies from 2 to 4 km; the height varies significantly, from 200 to 600 m.

The ridges often merge into larger massifs of various orientations of 20 km long and 12 km wide. Ridges and massifs are separated from each other by depressions varying in width from 3 to 5 km. A characteristic peculiarity of the relief is the presence of a large number of ring structures that can be interpreted as calderas. They are from 2.5 to 5 km across at a bottom depth of up to 450 m.

The analysis of the relief showed that the strike of the abyssal hills along the eastern and western flanks of the rift valley corresponds to the extension of the rift valley axis and does not correspond to the orientation of the echelon-like structures that were formed in the rift valley itself. According to this and the interpretation of linear magnetic anomalies, it can be assumed that the kinematics rearrangement occurred recently, 0.8–1 Ma ago. In the area of 49.25° N and 28.46° W, the fault scarp of the western side of the rift valley cuts off previously formed rift-related mountains.

*TMS-5, between 48.9° N
and the Maxwell Fracture Zone*

The boundary between TMS-4 and TMS-5 runs along the sublatitudinal linear depression at 48.9° N. Here, there are no signs of the rift valley displacement, although a change in the structural pattern is without

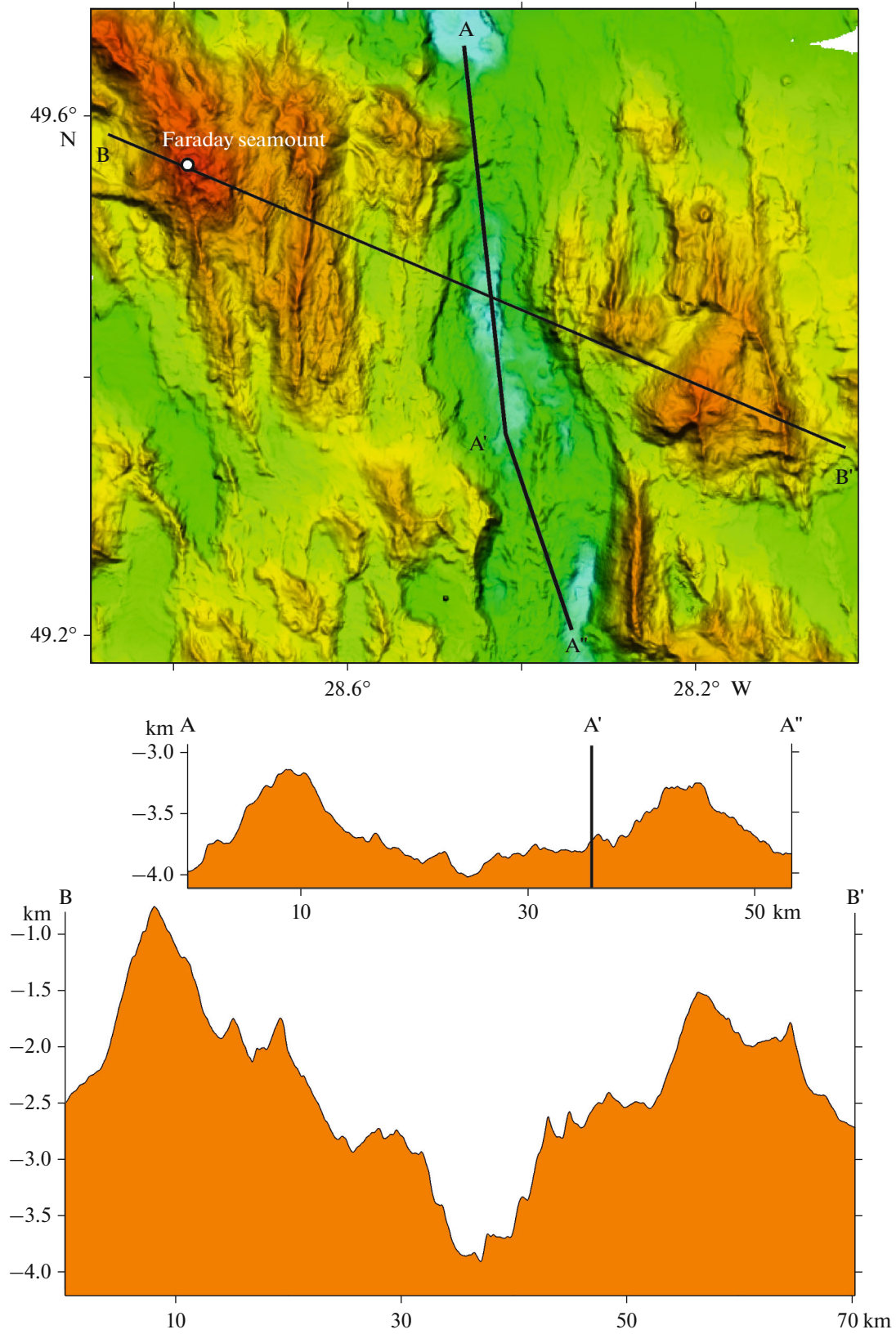


Fig. 8. The oceanic bottom topography and profiles in the TMS-4 area.

questions. As well, as shown by the sampling results, a small rise on the eastern side of the rift valley centered at 48.97° N and 27.97° W is composed of ultramafic rocks.

TMS-5 is fundamentally different from segments discussed above. In the southern part of the TMS-5, the rift valley is blocked by a large volcanic edifice at latitude 48.4° (Fig. 9, profile A–A').

The dome-shaped volcanic edifice consists of two conjugate volcanic uplifts, elongated perpendicular to the rift valley and separated from the structures of the older abyssal hills ridges by linear depressions. The dome is 17-km long and 10.6-km wide. The lava flows can be traced for a distance of up to 16 km from the center of the volcanic dome. The summit plane is located at a depth of 1600 m. The dome includes several craters.

According to dredging data, the dome is composed of slightly altered basalts, the most fresh of which were sampled from the western slope of the dome. In this regard, it can be assumed that rift volcanism and the spreading axis are shifted at present to the area of the western linear depression.

A rift valley (15–17 km wide, up to 4000 m deep) with a strike of 2° approaches the central part of the dome from the north. On the bottom of the valley are several parallel volcanic ridges up to 6 km long and up to 100 m high. They extend following the strike of the rift valley. The valley is asymmetrical (see Fig. 9, profile B–B').

The western slope is relatively flat (4°–5°) and consists of numerous fault benches. The eastern side is steep (19°–20°). It is a single fault plane with a drop amplitude of 150–300 m, which can be traced from north to south for a distance of at least 25 km.

To the south of 48.7° N, the depth and width of the rift valley gradually decrease, becoming wedge-shaped. South of the dome, only a small fragment of the rift valley is observed. It is expressed in relief as an isometric depression 14 km wide and up to 3700 m deep.

From the west and east it is bounded by stepped steep slopes (15°–25°). To the south, the rift valley is probably bounded by the Maxwell Fracture Zone [23]. There are no data on the seafloor topography for this area.

The flank zone of the TMS-5 has a typical ridged topography of abyssal hills. The width and height of the ridges vary considerably, from 2 to 9 km and from the first hundred meters to 1500 m, respectively. The distance between the ridges also varies.

On the eastern flank, in the area of 48.4° N and 27.5° W, the ridges merge, forming a large massif with ridged relief, separated only by small V-shaped ravines. There are also large depressions up to 4-km wide with a U-shaped transverse profile and a leveled bottom. All structures have meridional strike, coinciding with that of the rift valley.

Despite the fact that the morphology of rift ridges indicates that they are fragments of basaltic oceanic crust, there are also deeper rocks, gabbros, within their boundaries (for example, in the lower part of the ridge, 48.63° N and 28.14° W). This confirms the significant impact of tectonic movements on the formation of TMS-5 structures.

SEISMOTECTONICS AND GRAVITY ANOMALIES OF THE STUDY AREA

A feature of the seismicity distribution along the MAR in the Faraday area is the formation of dense clusters of shallow seismic events and their virtually complete absence in a number of segments (Fig. 10).

Seismic shallow events rarely occur in the rift valley of the MAR between 51.8° and 50.3° N. The only exception is the segment located between 51.2° and 51° N, a cluster of shallow events in which has a magnitude of $M \geq 4$. In the same segment, a certain number of deep-focus events are observed on the MAR flanks, 30–40 km from its axis. They form a pseudolinear group with the same orientation as the nontransform displacement in the TMS-2.

Shallow seismicity is most widespread within the rift valley and on its sides including both spreading cells with basalt volcanism, caused by the rise of heated matter and nontransform displacement, where, according to the analysis of the morphology of the bottom topography and dredged rocks, tectonic movements occurred. Moreover, shallow events with a small magnitude of $0 > M \leq 4$ are characteristic of sub-surface tectonic processes.

Deep-focus seismicity is concentrated mainly along the most extended segment with oblique spreading between 50.8° and 50.4° N. The nature of deep-focus seismicity may be associated with the appearance of deep detachment faults with a shear component that change the dynamics of extension in this segment. This can occur when the direction of plate divergence does not coincide with the direction of spreading, or when there is a difference in spreading rates to the south and north of the TMS-2–TMS-3 boundary. The cause of both possible cases is the irregular kinematics of movement at this part of the drifting plates on both sides of the MAR axis.

The analysis of seismic events with solutions for the source mechanisms according to [19, 20, 27] shows that mechanisms of lithospheric extension are mainly manifested along the MAR axis.

Shear mechanisms are manifested only on the western flank of the MAR at the TMS-2–TMS-3 boundary, at a distance of up to 100 km from the axis. This supports our interpretation of the spatial relationship between nontransform displacement and deep-focus seismicity. According to this interpretation, the configuration of the MAR has been transforming that leads to the development of a new transform displace-

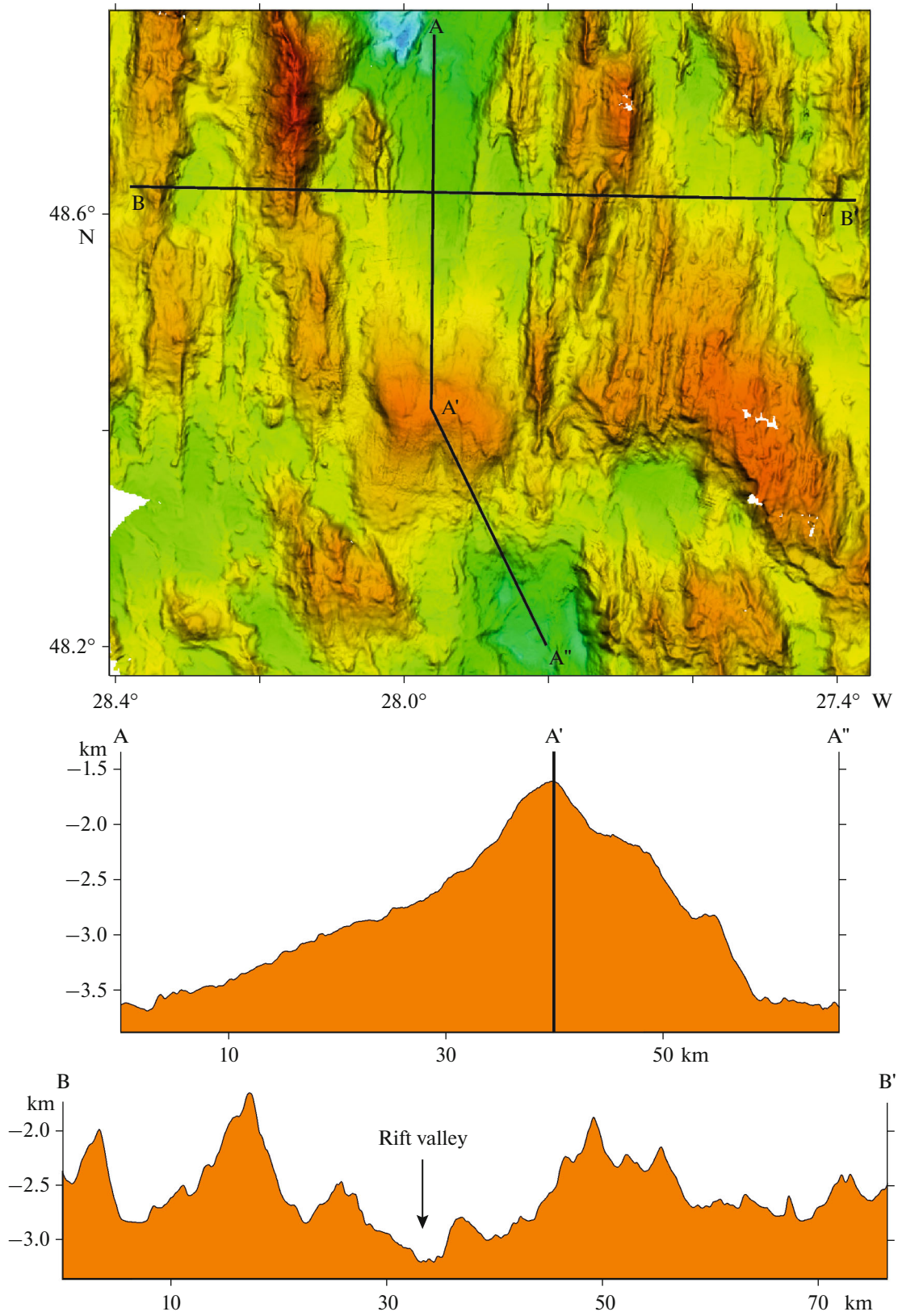


Fig. 9. The oceanic bottom topography and profiles in the TMS-5 area.

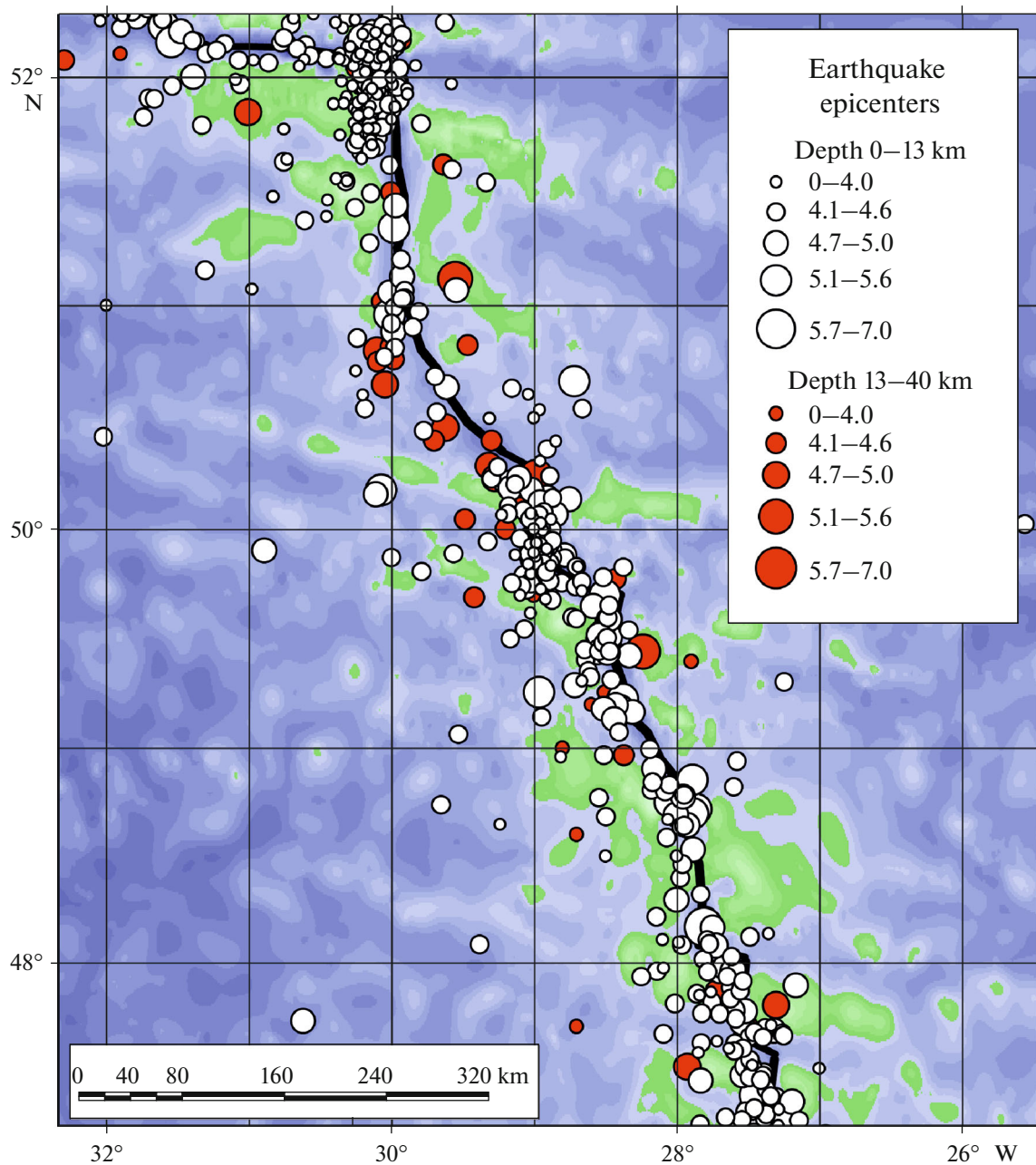


Fig. 10. The MAR seismicity (based on the data from [40], with amendments and additions). Circles show the position of earthquake epicenters and their magnitudes at different depth intervals (scale); MAR axis (black line).

ment. In addition, the signs of thrust kinematics with submeridional vergence were established at the same distances on the eastern flank. All of this points to the complex geodynamic situation in the area of study.

Gravity anomalies reflect the density structure of the crust and upper mantle. With some assumptions, low values correspond to areas with a thicker crust composed of a lower-density rocks (basalt). Accordingly, high values correspond to a less thick crust composed of denser rocks (ultramafic rocks). Average-density mani-

festations correlate with uplifts, composed of basalts, dolerites, and gabbros [12].

The axial part of the MAR has a complex mosaic configuration of Bouguer gravity anomalies (Fig. 11).

The low reduction values typical of the axial part of the MAR vary greatly in width and amplitude. The maximum width and amplitude were established in the northern part of the Faraday area (TMS-1) within Northern and Southern blocks, as well as in the southern part of the region (TMS-5), where the volcanic

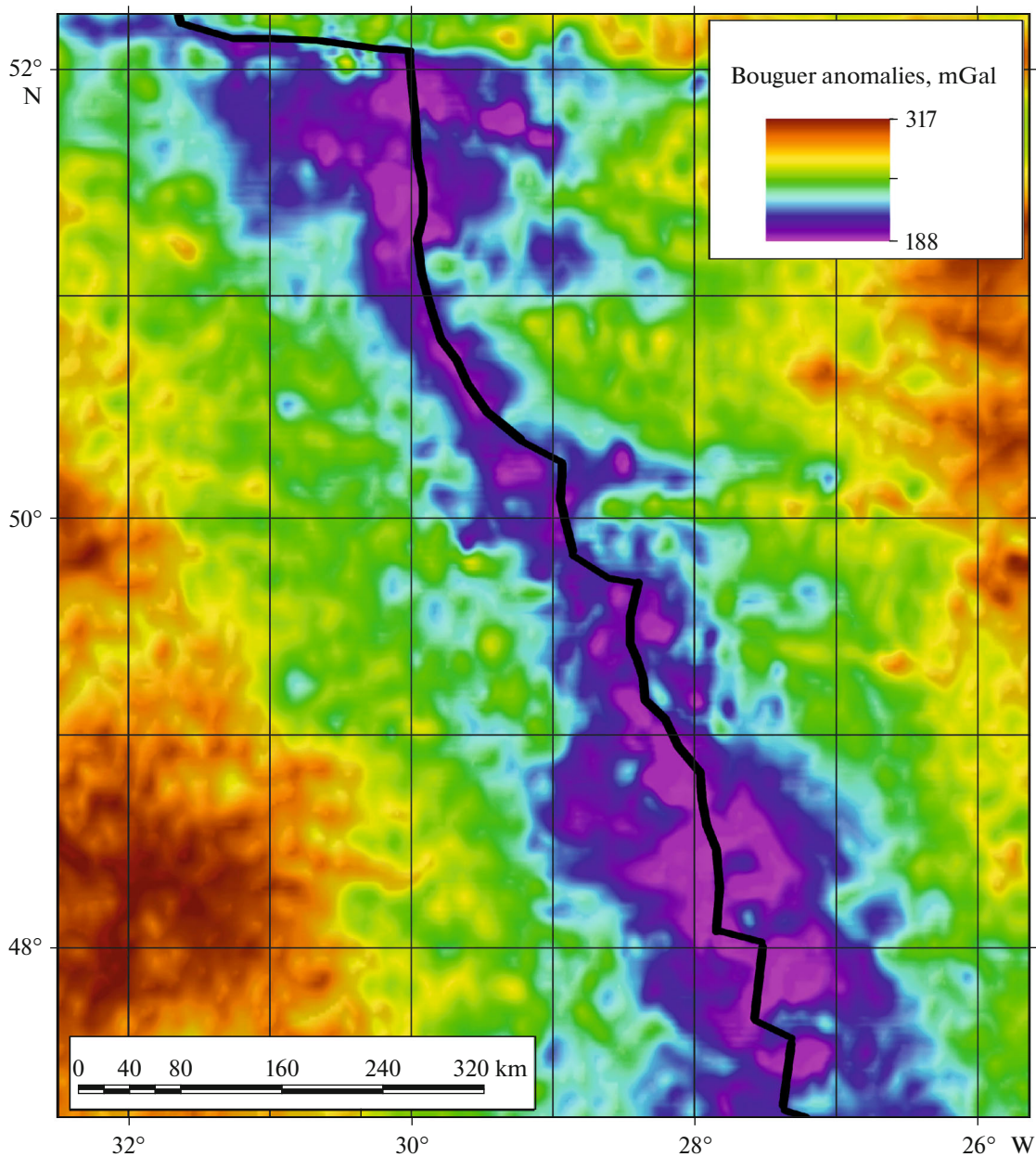


Fig. 11. Bouguer anomalies, calculated based on satellite altimetry data (after [34]) and the bottom topography (after [23]) on a $1' \times 1'$ grid. The MAR axis is shown by a black line.

uplift in the axial part of the MAR is so large that it actually overlaps the rift valley. In addition, this indicates a clear feedback between the productivity of magmatism and the intensity of the Bouguer axial anomaly.

As well, it should be noted that in areas with intense negative gravity anomalies, the deep-focus seismic events are manifested insignificantly (see Fig. 10).

The higher Bouguer anomaly values are noted in the area of ND 51.6° . Moreover, they are more pronounced to the east of the rift valley. Maxima are

observed above isometric elevations in the area of 51.1° N and 29.6° W.

In the anomalous gravity field, the structures of latitudinal uplifts at 50.1° N are clearly manifested. Moreover, higher values are noted over the Eastern Ridge than over the Western one. This is well correlated with the dredging data and emphasizes the structural and compositional asymmetry of the MAR, but the entire section of the rift valley between 49.9° and 49.7° N, judging by the anomalies, is characterized by thinned crust.

THE MAGNETIC FIELD AND AGE OF THE OCEANIC CRUST

Submeridional alternating linear anomalies are traced in the Faraday area. The range of anomalies is, on average, 800–1000 nTl. The positive anomalies are +400...+600 nTl, the negative ones are –400...–500 nTl. The revealed anomalies are arranged symmetrically relative to the central anomaly and correlate well from profile to profile, forming a system of spreading-related linear magnetic anomalies characteristic of this region of the Atlantic [32].

The central anomaly corresponding to the Brunhes geomagnetic epoch (0–0.78 Ma) extends across the entire region in a submeridional direction, winding and changing the strike azimuth from meridional to 315°–320°. Its position practically follows the outlines of the rift valley, which is obvious when combining magnetic and bathymetric data (Fig. 12).

Anomaly 2 (negative 0.78–4.19 Ma) including the anomaly 2A (positive 2.58–3.6 Ma) is traced conformably on both sides of the rift. These anomalies have characteristic outlines. Due to this, they can be sufficiently well identified, which made it possible to calculate the spreading rates of the area. The highest values of the magnetization intensity of the central anomaly are noted in TMS-1 and TMS-5. This is natural, since these are the only two spreading segments of the MAR that are characterized by the formation of the thick oceanic crust due to the outpouring of large volumes of basalt melt on the seafloor surface.

The spreading rate within the polygon remains stable (10–12 mm/year), which is especially typical of the western flank of the MAR within the study area. Moreover, this rate regularly decreases from 12 mm/year in the north to 9.7 mm/year in the south, on the western flank. This favors a rather stable tectonic situation on the western flank of the MAR within the study area. A more complex situation occurs on the eastern flank of the rift valley, where the average rate of the rifting is slightly higher (12–13 mm/year) than in the west, with its greater variability.

In the area of the sublatitudinal ridge (50°–50.33° N) a noticeable weakening of intensity until the complete disappearance of the central anomaly is observed.

At the latitude of 49.9° N, the central anomaly splits into two branches, one of which rests from the south on the Western latitudinal ridge and the other offsets 20 km to the east and is traced to the northeast up to 50.3° N. This fixes a jump of the spreading axis in the east direction, which, however, did not lead to the formation of a transform fault. In the future, it is possible that the entire section of the rift valley from 28.28° W at 50.1° N will shift to the west. There is no evidence that the western branch has now ceased to be active. This probably explains the reduced spreading rates in the region of 50.42°–50.27° N. The crust, which had an age and reverse magnetization corre-

sponding to the beginning of the second anomaly, was partly processed due to the drift of the rifting axis.

A similar situation is observed in the south of TMS-5, in the area of 48.33°–48.67° N. The central anomaly becomes wider and splits into two branches that converge south of the dome-shaped uplift. According to the dredging data, the western branch is the youngest, while the eastern one has ceased to be active.

Figure 13 shows the results of the fitting of magnetic anomaly sources for profile 10 (see Fig. 12) using the original technology for the 2D inverse magnetometry solution, previously used to model the magnetic layer within the rift system of the White Sea and the Kuril Island Arc [1, 3].

This technology is based on an iterative process that combines an interactive selection of processing technology and performing inversion steps with calculations following the selected algorithms. A researcher does not influence the specific details of the obtained models, since he determines only the general parameters of the computational scheme: the dimension of the task, the thickness and type of restrictions on required parameters, the degree of smoothness of solutions, degree of convergence, and error sensitivity, etc. A so-called procedure “case study” for verifying the adequacy of the solution algorithm under these specific conditions is provided and, as a rule, performed for each specific profile. The obtained preliminary solution is approximated by a simple block model for which a direct task is solved. Random noise is added to the obtained model data and they are fed to the input of the main inversion algorithm.

With the successful recovery of a simple block model, the resulting set of parameters is transferred to the inverse scheme for real data. In case of failure, the procedure of interactive iterative selection of the required parameters of the computational scheme is performed.

As a result, we obtain stable contrast distributions of magnetization in the selected or the given area of propagation of anomalous magnetic field sources with the involvement of a priori information and minimal influence of the subject opinions of the researcher on the solution.

The solution we obtained has a number of interesting features.

First, an alternation of subhorizontal blocks of normal and reverse geomagnetic polarity corresponding to the observed symmetrical pattern of the distinguished linear magnetic anomalies 1, 2, and 2a is observed on both sides of the central rift anomaly in the upper part of the section (Fig. 13). The boundaries between these blocks are not as clear as those of standard models of a bipolar magnetic layer, commonly used in magnetic geochronology [24].

In our opinion, this indistinctness of the interblock boundaries supports the solution we have found,

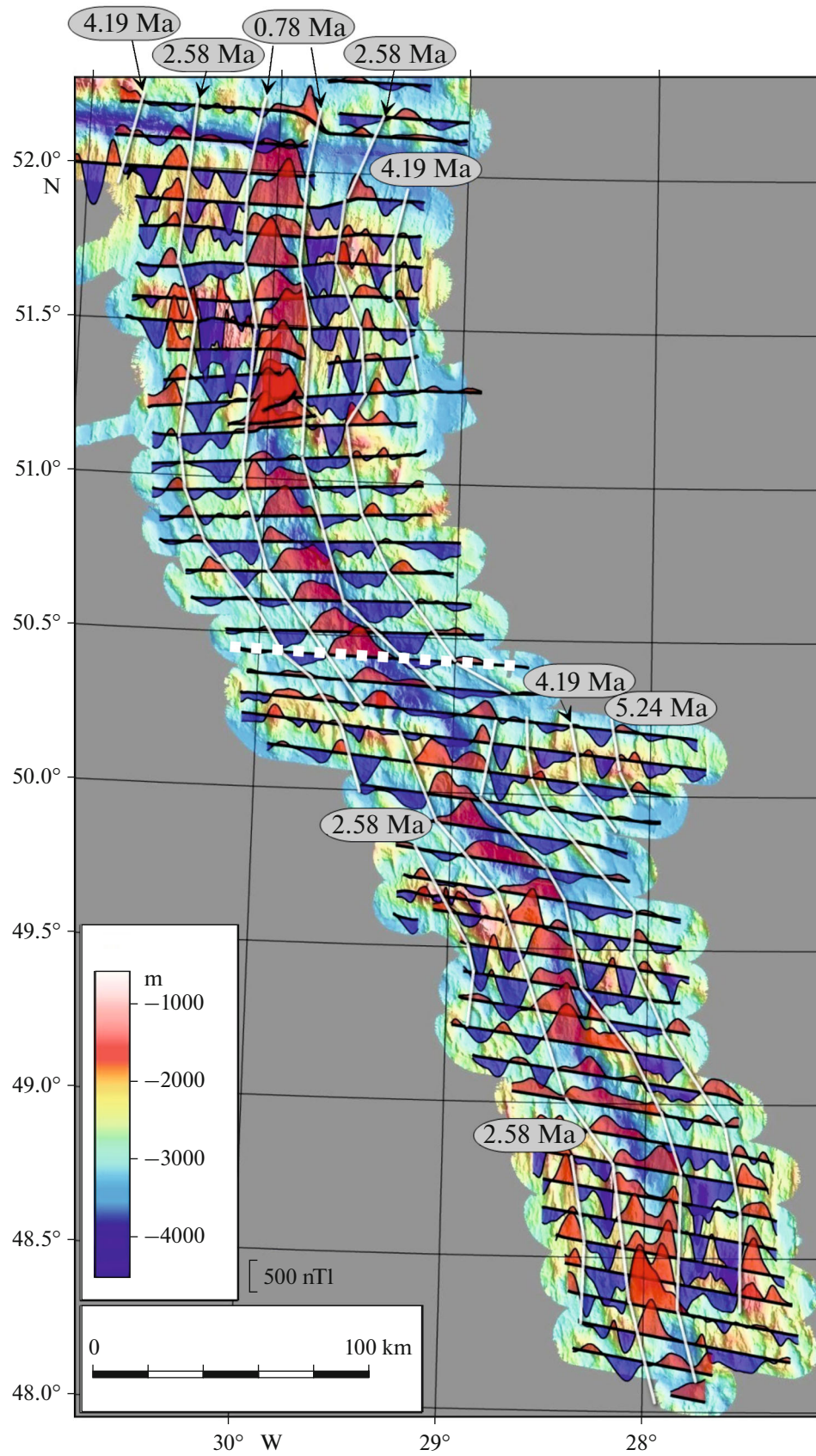


Fig. 12. The magnetic anomaly maps, superimposed on the bathymetry map of sea bottom. Figures shows isochrones (solid white lines); profile 10 (white dashed line); age of the crust (figures in ovals), according to distinguished linear magnetic anomalies.

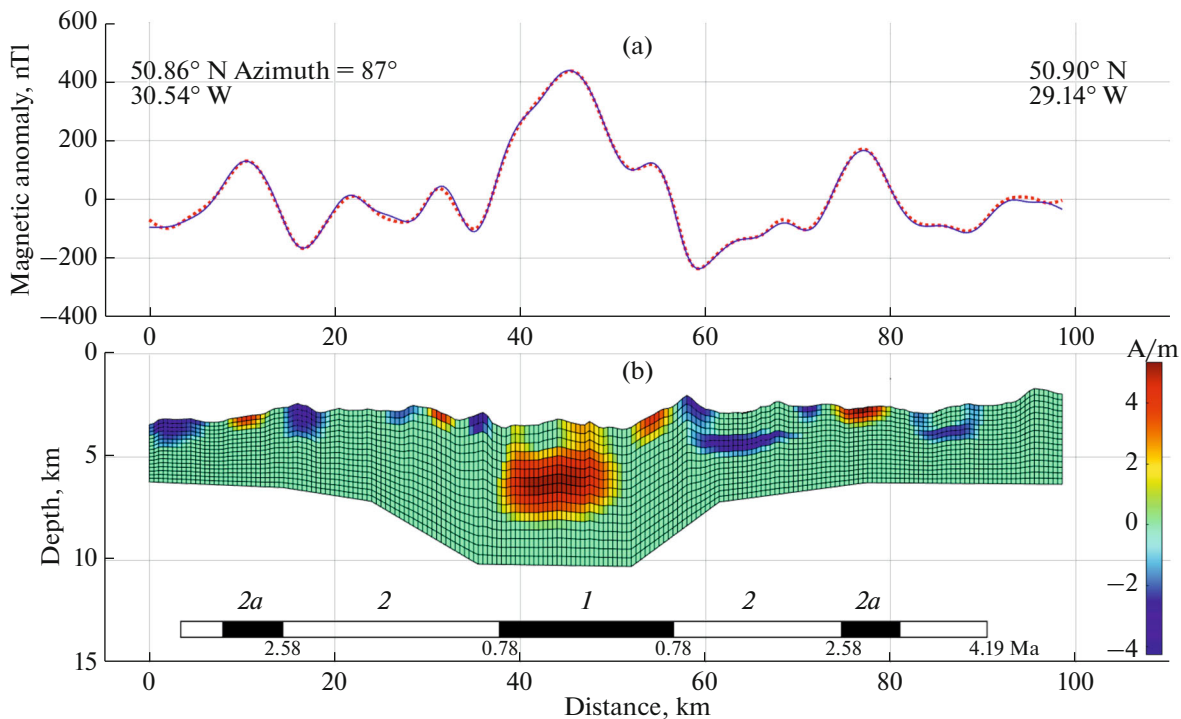


Fig. 13. A model for solving the inverse problem of magnetometry in a two-dimensional version by calculating the magnetic layer for the profile 10 of the Faraday area. (a) The anomalous magnetic field: measured (solid blue line), fitted (red dashed line), error of fitting was $<0.5\%$ of AMF amplitude; (b) the pattern of a magnetic layer: sizes of an elementary sell do not exceed 0.5 km in both dimensions, the magnetic polarity chrons fitted by magnetization (below) with numbers of anomalies and age (Ma). The profile 10 (white dashed line) is shown in Fig. 12.

since, according to [24], the process of inversion of the Earth's magnetic field takes a significant time on the geological scale. Consequently, the transition zone between normal and reverse polarity blocks in the spreading lithosphere can be extended, up to several km at spreading speeds, characteristic of the MAR.

Second, apart from the traditionally distinguished thin magnetic layer in the upper part of the section, a thick (3×10 km) magnetic body directly under the rift valley, in the depth range of 3–5 km below the bottom level, corresponds to the central anomaly. In this area, a magma chamber is usually placed in conventional models of rift zones near spreading ridges. This zone is distinguished by geophysical methods based on locally reduced density and propagation velocity of seismic waves.

We note that serpentinized mantle peridotites beneath the rift valley in areas of reduced volcanic activity will have a similar set of reduced values of physical parameters.

Therefore, the question of the presence of a particular structure beneath the rift valley could be solved on the basis of heat flow and temperature gradient data. If the temperatures are higher than the Curie temperature of serpentinites ($\sim 595^\circ\text{C}$), then, the proposed model should be incorrect; if they are lower, then it may be correct. There are no published results of heat flow measurements in this segment of the MAR. The

serpentinite model is supported by a significant number of mantle ultramafic rocks samples dredged on the Faraday area, which is typical of the spreading segments of the MAR with signs of dry spreading.

Third, in the eastern part of the section, we found fragments of a magnetic (apparently basalt) layer due to the conformability of the seafloor surface and low thickness, corresponding to anomaly 2 (reverse magnetic polarity), overlain by a 1.5-km layer of nonmagnetic rocks (see Fig. 13).

Since significant sedimentary deposits near the axis of the MAR are absent in this area of the Atlantic region, we have the right to assume that the magnetic interval of the basalt layer is located below the seafloor surface due to some factors or that these anomalies are not directly related to basalts.

The formation of serpentinites at the depth of the distinguished anomaly may be considered a variant of interpretation of this geometry of sources. This assumption is also consistent with the abundance of dredged mantle rocks in the Faraday polygon area and the same depth of the upper boundary of these anomalies and the axial anomaly.

DISCUSSION

According to our research, the considered area located to the south of the Charlie Gibbs Fracture

Zone is characterized by extremely diverse morpho-structures, which formation occurred during the interaction of volcanic and tectonic factors caused by both the features of stress fields within the lithospheric plates and structural-compositional and thermal heterogeneities within the axial zone of the MAR.

The Northern tectonomagmatic segment (TMS-1) has the simplest structure. Here, orthogonal spreading in two identically constructed spreading cells separated by the nontransform displacement is manifested. According to the data we obtained, a normal oceanic crust section with a thick basalt layer is formed in this area. There is a stable system of large rift ridges similar in morphology both on the western and eastern flanks. The presence of these ridges confirms the stability of mantle upwelling processes during 4 million years (since the Pliocene).

Another segment with active volcanic processes and abnormal morphology was found in the southernmost part of the Faraday area (TMS-5). In fact, a large dome-shaped uplift composed of basalts according to dredging data completely overlaps the rift valley. This single, but local, structure formed during a single powerful burst of volcanism activity. The latter has terminated, because the dome-shaped structure is separated from the more ancient abyssal hills by linear depressions formed during extension in the rift valley. At present, the axis of extension and volcanism is traced to the west of the dome. According to magnetic data, the axis of extension passed to the east of the uplift.

On the eastern flank, at a distance of about 30 km from the axis of the rift valley, there is a similar volcanic edifice, which, based on the interpretation of linear magnetic anomalies, has been formed over the past 1–2 Ma. Thus, it is possible to note that cycles of volcanic bursts alternated with long breaks. It seems unlikely that there are long-lived large magmatic chambers under the MAR. Therefore, it is possible that volcanism bursts are associated with the cyclical flow of more heated mantle matter from the deep horizons of the Earth in the form of “drops” that accelerate the processes of partial melting and lead to the outpouring of large volumes of basalt melt. During the period when additional thermal energy is not supplied, spreading comes to a state characteristic of slow-spreading ridges.

Between 51.2° and 50.2° N the rift valley changes its strike from the meridional to the southeastern. At the same time, the internal structures of the rift valley are still oriented meridionally, forming a system of depressions and neovolcanic rises, which is characteristic of the kinematic system of oblique spreading. The latter is accompanied by the formation of normal and strike-slip faults within the rift valley and on its sides, the length and strike of which depend on the angle between the direction of spreading and the extension of the rift valley axis.

In the North Atlantic, oblique spreading structures are characteristic of the Mohn and Knipovich ridges located to the north [4, 35]. Meridional structures are also present on the flanks of the rift valley at a distance of up to 25 km. Older structures, however, have a strike close to that of the axis of the rift valley, which confirmed the change in the structural setting that occurred ~2.5 Ma ago.

It should be noted that this entire arc-shaped segment is characterized by a low-ridge topography, which is atypical for volcanism of normal spreading cells. Judging by the magnetic anomalies of average intensity and Bouguer anomalies, the basalt layer has a low thickness here. The difference in elevation between the rift valley bottom and the ridges on the flanks does not exceed 1000 m. It can be assumed that such a relief is formed due to development of numerous low-amplitude nontransform offsets without the formation of large rift ridges in an environment of latitudinal extension with an additional shear component.

As a rule, it is believed that the depth of the rift valley directly depends on the volumes of rising basalt melts [2, 29, 37]. In areas with elevated temperatures beneath the MAR axis, large volumes of basalt melt are formed and, subsequently, come to the surface, leading to a decrease in the depth of the rift valley. Accordingly, the colder the mantle beneath the MAR, the deeper the rift valley.

According to the results of our research, the depth of the rift valley in the areas of sublatitudinal linear uplifts of the Faraday area (50.1° and 49.5° N) is sharply decreasing, despite the fact that they are composed largely of deep-seated rocks. It means that the mantle in this area is cold. Thus, other factors related to tectonic processes can have a significant impact on the depth of the rift valley.

In the Faraday area, the segments where the rift valley has a meridional strike alternate with those whose strikes change to the northwest. The transition from one strike to another occurs without displacement of the rift valley, which is typical of ND. The latter are zones where horizontal shear stress relief occurs with the formation of small normal faults and faults with extensional component.

There are no signs of extended linear sublatitudinal shifts with displacement of the rift valley characteristic of the active parts of transform faults. The variety of morphotectonic manifestations of nontransform displacements indicates that they form due to variations in some conditions, including stress fields, kinematic characteristics of plates and rock rheology.

The peculiarity of the Faraday area is that everywhere (with the exception of TSM-1), both directly at the sides of the rift valley and on the flanks, at a considerable distance, there are massifs (usually isometric forms), in which deep rocks are brought to the surface, in various percentages with basalts and dolerites, representing the lower crust (rocks of the lay-

ered complex, mainly various gabbros) and deeper rocks (serpentinized dunites and peridotites), which were originally located in the upper mantle.

Almost all deep rocks bear signs of intense tectonic deformations associated with their uplift into the upper crustal horizons, up to their appearance on the bottom surface. Such structures are characteristic of segments of the MAR with a low spreading rate of a specific structure (the Sierra Leone, Cape Verde and other fracture zone areas), where their formation is associated with the existence of anomalous areas with very small volumes of basalt melts that came to the surface during dry spreading. In the North Atlantic, such structures have not been previously known.

The massifs vary in morphology, but the most common structures are those with a low-angle slope facing the rift valley and a steeper opposite slope. The slope surfaces facing the rift valley sometimes have corrugated surfaces (as in the area of 51.1° N and 29.5° W).

It is believed that such massifs (oceanic core complexes) were formed during the exhumation of deep-seated rocks along low-angle faults within the sides of rift valleys. However, the dredging of the structures of the Faraday area revealed that the morphology of uplifts composed of deep-seated rocks can be very diverse:

- (i) smoothed rounded high;
- (ii) isometric massifs of any strike;
- (iii) narrow linear ridges with irregular slope steepness (slopes facing the rift valley may be much steeper than the opposite ones).

The irregular slope steepness can be formed due to the frequent change of the polarity of the faults bounded the rift valley, which leads to the conservation of fault planes with close slope angles on both sides of the uplifts [15]. Rounded highs, as a rule, are composed of deep-seated rocks and are associated with the subvertical uplift of ultramafic rock massifs.

Serpentinization is a low-temperature isothermal process that leads to a significant increase in volume of the source rocks and their uplift/extrusion to the seafloor surface.

It is known that serpentinites are very plastic rocks that begin to flow under a light load. They penetrate through weakened zones and cracks into the overlying and adjacent rocks, separating them into blocks. Later, they move randomly, both laterally and vertically, forming a specific small-block chaotic relief of serpentinite melange during destruction (at least on land).

It can be assumed that similar mechanisms operate in the upper horizons of the oceanic crust of the Faraday area, leading to a turn and inclination in any direction of the crustal blocks and the formation of a chaotic tectonic topography.

Structures composed mainly of serpentinized ultramafic rocks are located on the eastern flank of the rift valley, while gabbros and dolerites are located mainly on its western flank.

Such asymmetry may be associated with the asymmetric structure of the rift valley. It means that during extension the gentlest faults, along which the relative displacement of the blocks of the newly-formed oceanic crust occurs, are located on the eastern side of the valley and have constant western vergence. Less gentle faults are confined to the western side of the rift valley. Due to this difference in kinematics and amplitude of tectonic movements, deeper-seated rocks crop out on the eastern side of the rift valley.

At latitudes of 50°, 49.5°, and 48.5°N, the rift valley becomes narrow. Its bottom rises from depths of 4300–4200 m to 3300–3200 m. The analysis of the topography shows that these areas correspond to large extended linear sublatitudinal ridges, consisting of closely arranged large isometric massifs, some of which run symmetrically on both sides of the rift valley.

Judging by their length (up to 200 km), they exist for a long period of time during the formation of the newly formed crust in the axial part of the MAR. A consistent rejuvenation of the massifs towards the rift valley has been revealed, where the process of uplifting deep-seated rocks to the seafloor surface still continues. All massifs are bounded by different-sized nontransform displacements.

As a rule, large linear structures largely composed of deep rocks are known as transverse ridges, i.e., structures located in the sides of the active parts of large transform faults and formed in the junction areas of rift and fracture zone valleys.

Within double fracture zones (for example, the Charlie Gibbs Fracture zone), when two fracture zone valleys are located close to each other, the inter-transform ridge may also represent a sequence of uplifts composed of deep-seated rocks [10, 38]. As shown, separate chaotically located massifs of deep-seated rocks can be formed within rift valleys, but in this case they do not form a single sequence in the form of extended ridges.

The peculiarity of the Faraday area is that the sublatitudinal ridges here are not confined to transform faults. They are located between nontransform displacements, which are not considered as large deep structures that control the formation of very specific linear uplifts for a long time.

The sublatitudinal ridges in the Faraday area are clearly traced based on high Bouguer anomaly values. It can be assumed that the roots of such high-density structures are traced to the basement of the lithosphere. Together with the boundary nontransform displacements, they are responsible for the existence of areas of a thick, cold lithosphere where magmatic cells with reduced generation of basalt melts are formed. It is probable that less extended and large structures only partly control the boundaries of magma-generating structures. Therefore, extended sublatitudinal ridges are not formed here.

CONCLUSIONS

(1) The Mid-Atlantic Ridge area between the Charlie Gibbs and Maxwell Fracture Zones is characterized by a significant reduction of volcanism, which leads to the uplift of lower crustal and upper mantle rocks to the seafloor. Isolated oceanic core complexes of various configurations, as well as extended sublatitudinal ridges, composed of deep rocks (ultramafic rocks and diverse gabbros) are formed.

The extension and spreading are continuous processes, while volcanism occurs at stages separated by long periods of calm. Judging by the length of the Western sublatitudinal ridge and the extrapolation of linear magnetic anomalies, this situation has existed for at least 14–16 Ma.

(2) The formation of most oceanic core complexes is associated not only with tectonic factors (drop of lithostatic pressure), but also with serpentinization of peridotites, which leads to a decrease in density, an increase in volume and, as a consequence, the uplift of large ultramafic massifs, including detached blocks of gabbros, dolerites and basalts. Numerous zones of sliding, crushing, abrasion, and deformation of rocks are signs of tectonic movements.

(3) Since the direction of divergence of the North American and Eurasian lithospheric plates is close to the sublatitudinal, the spreading in the rift valley in sectors with meridional and northwestern strike occurs in different ways. In NW-striking sectors, subparallel linear oblique structures are formed with respect to the direction of spreading. Their morphology is diverse, ranging from echelon-shifted spreading axes bounded by parallel depressions or linear neovolcanic rises, echelon ledges with overlapping ends and oblique shear zones with extension basins located at an angle to the axis of the rift valley.

(4) The Faraday area is characterized by numerous nontransform displacements of different amplitudes that formed when the relative displacement of segments of the oceanic lithosphere occurs in wide areas under shear and extension conditions rather than in the form of local zones of displacement of the oceanic lithosphere along transform faults. At the same time, numerous local low-amplitude strike-slip and normal fault structures are formed.

(5) Tectonic factors determine the morphology of the forming tectonomagmatic structures of the study region. One exception is the case where the volumes of basalt melts that come to the surface in a short period of time are significantly higher than the average volumes for this segment of the rift valley, as in the region of 48.4° N.

(6) The analysis revealed the presence of heterogeneous sources of magnetic anomalies within the study region. These are usually of a volcanic origin, but may also be associated with serpentinized ultramafic rocks.

ACKNOWLEDGMENTS

We are grateful to the crew of the R/V *Academik Nikolaj Strakhov* (Russia) and the entire expedition team for their comprehensive assistance in expedition research during the 53rd cruise in 2022. The authors are grateful to the anonymous reviewers for useful comments and to the editor for comprehensive editing.

FUNDING

This work was carried out within the framework of the state assignments FMMG-2022-0003, FMMG-2023-0005, FMWE-2021-0005.

CONFLICT OF INTEREST

The authors declare that they have no conflicts of interest.

REFERENCES

1. A. S. Baluev, Yu. V. Brusilovskii, and A. N. Ivanenko, "The crustal structure of Onega–Kandalaksha paleorift identified by complex analysis of the anomalous magnetic field of the White Sea," *Geodynam. Tectonophys.* **9** (4), 1293–1312 (2018).
2. L. V. Dmitriev, S. Yu. Sokolov, and A. A. Plechova, "Statistical assessment of variations in the compositional and P-T parameters of the evolution of mid-oceanic ridge basalts and their regional distribution," *Petrology* **14** (3), 209–229 (2006).
3. N. A. Pal'shin, A. N. Ivanenko, and D. A. Alekseev, "Inhomogeneous structure of magnetic layer of the Kuril Island Arc," *Geodynam. Tectonophys.* **11** (3), 583–594, 2020.
4. A. A. Peyve, "Accretion of oceanic crust under conditions of oblique spreading," *Geotectonics* **43** (2), 87–99, 2009.
5. A. A. Peyve, K. O. Dobrolyubova, V. N. Efimov, et al., "Geological features of the Sierra Leone Fracture Zone Region, central Atlantic Ocean," *Dokl. Earth Sci.* **377** (3), 310–313 (2001).
6. A. A. Peyve, G. N. Savel'eva, S. G. Skolotnev, and V. A. Simonov, "Tectonics and origin of the oceanic crust in the region of "dry" spreading in the central Atlantic (7°10'–5° N)," *Geotectonics* **37** (2), 75–94 (2003).
7. A. A. Peyve, S. Yu. Sokolov, A. N. Ivanenko, et al., "Accretion of the oceanic crust in the Mid-Atlantic Ridge (48°–51.5° N) during "dry" spreading," *Dokl. Earth Sci.* **507**, S349–S356 (2022).
8. Yu. M. Pushcharovskiy, A. A. Peyve, Yu. N. Raznitsin, et al., "The Cape Verde Fracture Zone, the Central Atlantic: Rock composition and structures," *Geotectonics* **22** (6), 485–495 (1988).
9. S. G. Skolotnev, A. A. Peyve, A. Sanfilippo, et al., "Peculiarities of the tectonomagmatic processes in the interaction area between the Icelandic Plume and the Bight Transform Fault (North Atlantic)," *Dokl. Earth Sci.* **504**, 233–239 (2022).
10. S. G. Skolotnev, A. Sanfilippo, A. A. Peyve, et al., "Geological and geophysical studies of the Charlie

- Gibbs Fracture Zone (North Atlantic),” *Dokl. Earth Sci.* **497** (1), 191–194 (2021).
11. M. Abelson and A. Agnon, “Mechanics of oblique spreading and ridge segmentation,” *Earth Planet. Sci. Lett.* **148**, 405–421 (1997).
 12. D. K. Blackman, J. P. Canales, and A. Harding, “Geophysical signatures of oceanic core complexes,” *Geophys. J. Int.* **178**, 593–613 (2009).
 13. J. R. Cann, D. K. Blackman, D. K. Smith, et al., “Corrugated slip surfaces formed at North Atlantic ridge-transform intersections,” *Nature* **385**, 329–332 (1997).
 14. M. Cannat, Y. Lagabrielle, H. Bougault, et al., “Ultramafic and gabbroic exposures at the Mid-Atlantic Ridge: Geological mapping in the 15° N region,” *Tectonophysics* **279** (1–4), 193–213 (1997).
 15. M. Cannat, D. Sauter, V. Mendel, et al., “Modes of seafloor generation at a melt-poor ultraslow-spreading ridge,” *Geology* **34** (7), 605–608 (2006).
 16. O. Dauteuil and J. Brun, “Oblique Oblique rifting in a slow-spreading ridge,” *Nature* **361**, 145–148 (1993).
 17. H. J. B. Dick, M. A. Tivey, and B. E. Tucholke, “Plutonic foundation of a slow spreading ridge segment: Oceanic core complex at Kane Megamullion, 23°30′ N, 45°20′ W,” *Geochem. Geophys. Geosyst.* **9** (5), 1–44 (2008).
 18. G. Thompson and W. B. Bryan, “Low angle faulting and steady state emplacement of plutonic rocks at ridge-transform intersections,” *EOS. Trans. AGU* **62** (1981).
 19. A. M. Dziewonski, T.-A. Chou, and J. H. Woodhouse, “Determination of earthquake source parameters from waveform data for studies of global and regional seismicity,” *J. Geophys. Res.* **86**, 2825–2852 (1981).
 20. G. Ekström, M. Nettles, and A. M. Dziewonski, “The global CMT project 2004-2010: Centroid-moment tensors for 13,017 earthquakes,” *Phys. Earth Planet. Inter.* **200–201**, 1–9 (2012).
 21. J. Escartin, C. Mevel, S. Petersen, et al., “Tectonic structure, evolution, and the nature of oceanic core complexes and their detachment fault zones (13°20′ N and 13°30′ N, Mid Atlantic Ridge),” *Geochem. Geophys. Geosyst.* **18**, 1451–1482 (2017).
 22. M. Fournier and C. Petit, “Oblique rifting at oceanic ridges: Relationship between spreading and stretching directions from earthquake focal mechanisms,” *J. Struct. Geol.* **29**, 201–208 (2007).
 23. GEBCO 15” Bathymetry Grid. Vers. 2019. <http://www.gebco.net> (Accessed September 1, 2022).
 24. J. S. Gee and D. V. Kent, “Source of oceanic magnetic anomalies and the geomagnetic polarity timescale,” *Treat. Geophys.* **5**, 455–507 (2007).
 25. E. Gracia, J. Charlou, J. Radford-Knoery, and L. Parson, “Non-transform offsets along the Mid-Atlantic Ridge south of the Azores (38° N–34° N) ultramafic exposures and hosting of hydrothermal vents,” *Earth Planet. Sci. Lett.* **177 P**, 89–103 (2000).
 26. N. Grindlay, P. Fox, and K. Macdonald, “Second-order ridge axis discontinuities in the south Atlantic: Morphology, structure, and evolution,” *Mar. Geophys. Res.* **13**, 21–49 (1991).
 27. Harvard CMT. Harvard University Centroid-Moment Tensor Catalog. <http://www.globalcmt.org/> (Accessed October 10, 2018).
 28. J. A. Karson, G. Thompson, S. E. Humphries, et al., “Along axis variations in seafloor spreading in the MARK area,” *Nature* **328**, 681–685 (1987).
 29. E. M. Klein and C. H. Langmuir, “Global correlations of ocean ridge basalt chemistry with axial depth and crustal thickness,” *J. Geophys. Res.* **92** (B8), 8089–8115 (1987).
 30. L. Lavier, W. R. Buck, and A. N. Poliakov, “Self-consistent rolling-hinge model for the evolution of large-offset low-angle normal faults,” *Geology* **27**, 1127–1130 (1999).
 31. R. C. Searle and J. F. Casey, et al., “Life cycle of oceanic core complexes,” *Earth Planet. Sci. Lett.* **287**, 333–344 (2009).
 32. S. Merkouriev and C. DeMets, “High-resolution Quaternary and Neogene reconstructions of Eurasia–North America plate motion,” *Geophys. J. Int.* **198**, 366–384 (2014).
 33. C. Mevel, M. Cannat, P. Gente, et al., “Emplacement of deep crustal and mantle rocks on the west median valley wall of the MARK area (MAR, 23° N),” *Tectonophysics* **190**, 31–53 (1991).
 34. K. Okino, D. Curewitz, M. Asada, et al., “Preliminary analysis of the Knipovich Ridge segmentation: influence of focused magmatism and ridge obliquity on an ultraslow spreading system,” *Earth Planet. Sci. Lett.* **202**, 275–288 (2002).
 35. D. T. Sandwell and W. H. Smith, “Global marine gravity from retracked Geosat and ERS-1 altimetry: Ridge segmentation versus spreading rate,” *J. Geophys. Res.* **114** (B1), 1–18 (2009).
 36. D. Sauter, M. Cannat, S. Roumejon, et al., “Continuous exhumation of mantle-derived rocks at the Southwest Indian Ridge for 11 million years,” *Nat. Geosci.* **6**, 314–320 (2013).
 37. J. Schilling, M. Zajac, R. Evans, et al., “Petrologic and geochemical variations along the Mid-Atlantic Ridge from 29° N to 73° N,” *Am. J. Sci.* **283**, 510–586 (1983).
 38. S. G. Skolotnev, A. Sanfilippo, A. A. Peyve, et al., “Seafloor spreading and tectonics at the Charlie Gibbs transform system (52°–53° N, Mid Atlantic Ridge): Preliminary results from R/V A. N. Strakhov expedition S50,” *Ofioliti* **46** (1), 83–101 (2021).
 39. B. Taylor, K. Crook, and J. J. Sinton, “Extensional transform zones and oblique spreading centers,” *J. Geophys. Res.* **99** (B10), 19707–19718 (1994).
 40. USGS Earthquake Composite Catalog, 2021. <https://earthquake.usgs.gov/earthquakes/search/> (Accessed February, 2021).
 41. T. Zheng, B. E. Tucholke, and J. Lin, “Long-term evolution of nontransform discontinuities at the Mid-Atlantic Ridge, 24° N–27°30′ N,” *J. Geophys. Res.: Solid Earth* **124**, 10023–10055 (2019).

Translated by D. Voroshchuk